[American Journal of Science, Vol. 318, June, 2018, P. 603–639, DOI 10.2475/06.2018.01]

American Journal of Science

JUNE 2018

ISOTOPE SCLEROCHRONOLOGY OF AMMONITES (*BACULITES COMPRESSUS*) FROM METHANE SEEP AND NON-SEEP SITES IN THE LATE CRETACEOUS WESTERN INTERIOR SEAWAY, USA: IMPLICATIONS FOR AMMONITE HABITAT AND MODE OF LIFE

NEIL H. LANDMAN*,†, J. KIRK COCHRAN**, MARIAH SLOVACEK*, NEAL L. LARSON***, MATTHEW P. GARB§, JAMIE BREZINA§§, and JAMES D. WITTS*

ABSTRACT. Ammonites, as well as other fauna, were common in methane seeps of the Late Cretaceous Western Interior Seaway (WIS) of North America. Biogeochemical processes at the seeps, in particular the anaerobic oxidation of methane, produced a dissolved inorganic carbon reservoir with a low $\delta^{13}C$, manifested in the carbon isotope composition of the inorganic calcium carbonate concretions associated with the seeps and recorded in well-preserved shells of ammonites documented at the sites. Detailed sclerochronological sampling of six well-preserved specimens of *Baculites compressus* collected at seep sites in the Pierre Shale of South Dakota reveals three patterns that can be explained by reference to two specimens of the same species collected at age-equivalent non-seep sites. Three of the specimens exhibit uniformly low values of $\delta^{13}C$ that are significantly different (unpaired t-test, $p < .0001$) from similarly sized specimens of the same species collected at age-equivalent non-seep sites, suggesting that these ammonites lived at the seeps during the time interval over which the shell was secreted (adult portion of the shell). Two of the specimens collected from a seep site exhibit values of $\delta^{13}C$ consistent with early ontogeny at a non-seep site followed by later ontogeny at a seep site. The values of $\delta^{18}O$ of all the specimens reveal water temperatures of 16 to 28 °C. One small juvenile (15 mm long) collected at a seep site exhibits higher values of $\delta^{13}C$ consistent with a non-seep environment, but values of $\delta^{18}O$ that indicate very warm or slightly brackish water, suggesting that this animal lived in surface waters during its early ontogeny and died soon after arriving at the seep. Our results demonstrate that seep fluids affected the geochemistry of the water column above the seeps and that seeps provided habitats for ammonites in the WIS. Thus, although ammonites were mobile animals, they probably exploited a low-energy life style, remaining at the same site for extended periods of time.

Key words: Upper Cretaceous, Pierre Shale, Western Interior Seaway, methane seeps, ammonites, *Baculites compressus*, sclerochronology, $\delta^{18}O$, $\delta^{13}C$

INTRODUCTION

"Tepee buttes" (so-called because they bear a superficial resemblance to the tepees of Native Americans) were first described by Gilbert and Gulliver (1895) in the

* Division of Paleontology (Invertebrates), American Museum of Natural History, New York, New York 10024, USA
** School of Marine and Atmospheric Sciences, Stony Brook University, Stony Brook, New York 11794, USA
*** Larson Paleontology Unlimited, Keystone, South Dakota 57745, USA
§ Department of Geology, Brooklyn College, Brooklyn, New York 11210, USA
§§ Department of Mining Engineering, South Dakota School of Mines and Technology, Rapid City, South Dakota 57701, USA
† Corresponding author: landman@amnh.org

Upper Cretaceous of the U.S. Western Interior along the Front Range of the Rocky Mountains in Colorado (figs. 1 and 2). They appear as conical hills or mounds and are composed of limestone, usually up to 60 m in diameter and 10 m in height. These features are now recognized as fossil methane seep deposits (Kauffman and others, 1996) and occur in the Upper Cretaceous Pierre Shale from central Montana to south-central Colorado, and from the Front Range of the Rocky Mountains to western Kansas (Bishop and Williams, 2000; Shapiro and Fricke, 2002; Metz, 2010; Landman and others, 2012, 2018; Larson and others, 2014). They range in age from middle Campanian to early Maastrichtian. Kiel and others (2012) have reported similar deposits from the upper Cenomanian Tropic Shale of Utah.

The seep deposits from the U.S. Western Interior contain a diverse assemblage of organisms including ammonites, bivalves, notably inoceramids and aggregations of lucinids (that presumably harbored chemosymbionts), gastropods, crinoids, crabs, echinoids, sponges, tube worms, chemoautotrophic bacteria, radiolarians, and foraminifera (Bishop and Williams, 2000; Landman and others, 2012; Larson and others, 2014; Meehan and Landman, 2016; Hunter and others, 2016). A total of 30 molluscan species were reported at single sites from middle-upper Campanian seep deposits in Colorado (Howe, ms, 1987). The diversity of organisms is higher at seep sites with extensive carbonate deposits, presumably because such deposits provided unique habitats for organisms that required hard substrates for attachment (Meehan and Landman, 2016).

Ammonites have been recorded in methane seep deposits in the Western Interior from the upper part of the middle Campanian to the lower part of the lower Maastrichtian (fig. 3). They span the *Baculites scotti/Didymoceras nebrascense* Zones, *D. stevensoni* Zone, *Exiteloceras jenneyi* Zone, *D. cheyennense* Zone, *B. compressus/B. cuneatus* Zones, and *B. eliasi/ B. baculus* Zones (Larson and others, 1997; Cobban and others, 2006; Larson and others, 2014). The diversity of ammonites varies depending on the ammonite zone. Five to eight ammonite species occur in each of these zones and represent the genera *Baculites, Didymoceras, Hoploscaphites, Nostoceras, Menuites, Placenticeras*, and *Spiroxybeloceras*. With few exceptions, the ammonite species are not restricted to the seeps but also occur elsewhere in the basin (Landman and others, 2013).

Landman and others (2012) and Cochran and others (2015) investigated the isotope composition of well-preserved ammonite shells from seep deposits in the Upper Cretaceous Pierre Shale of South Dakota. They documented low $\delta^{13}C$ values, presumably derived from anaerobic oxidation of methane that imprinted the dissolved inorganic carbon reservoir and was incorporated into the ammonite shells during growth. They hypothesized that the ammonites spent part of their lives at the seeps. However, their sampling was limited to one or a few samples from each specimen. Low values of $\delta^{13}C$ have also been measured in ammonite shells from the Upper Cretaceous (Maastrichtian) López de Bertodano Formation of Seymour Island, Antarctica (Tobin and Ward, 2015; Ivany and Artruc, 2016). Tobin and Ward (2015) attributed this to an increased contribution of metabolic C in ammonites in later ontogeny relative to the higher $\delta^{13}C$ observed in co-occurring bivalves and gastropods, but it is difficult to ascribe some of the lowest values of $\delta^{13}C$ that they measured in ammonite shells (ranging from $-7‰$ to $-20‰$) to this explanation. Indeed, Little and others (2015) documented shallow water hydrocarbon seeps in the López de Bertodano Formation, and Tobin and Ward (2015) acknowledged the possibility of a methane seep contribution to the $\delta^{13}C$ signature of the ammonite shells from this locality. Here, we further explore the hypothesis that methane seeps provided a habitat for ammonites. We test the hypothesis through sclerochronological analyses of excellently preserved shell material from seep and age-equivalent non-seep specimens of *Baculites compressus*,

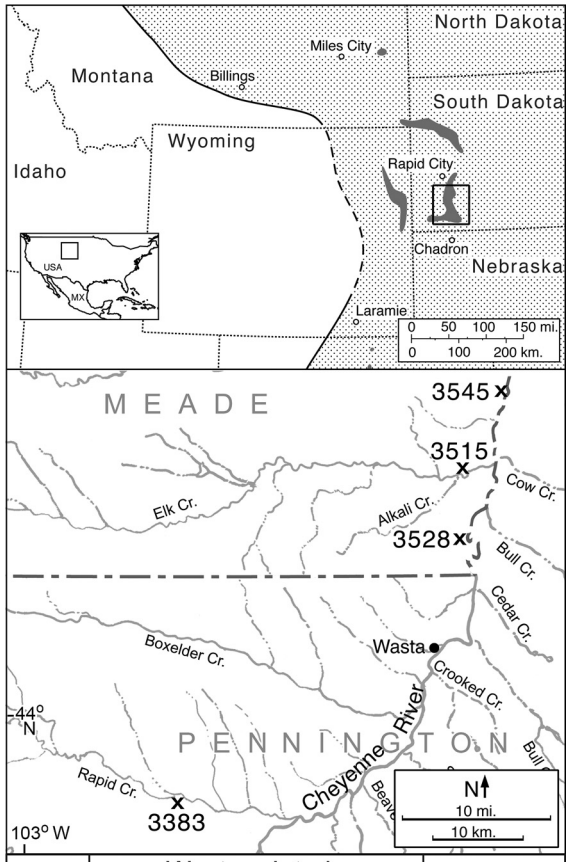

Stage	Western Interior Ammonite zones	Age (Ma)
lower Maas.	*Baculites baculus*	
upper Campanian	*Baculites eliasi*	72.50±0.31
	Baculites jenseni	
	Baculites reesidei	73.41±0.46
	Baculites cuneatus	
	Baculites compressus	73.79±0.36 73.70±0.13 74.05±0.39
	Didymoceras cheyennense	75.21±0.15
	Exiteloceras jenneyi	74.67±0.12 75.62±0.11
	Didymoceras stevensoni	75.16±0.12
	Didymoceras nebrascense	75.74±0.28
mid Camp.	*Baculites scotti*	75.56±0.11 75.84±0.26

Fig. 1. Top. Map showing methane seep in the middle-upper Campanian and Maastrichtian Pierre Shale in South Dakota, Wyoming, Montana, and Nebraska. The dark patches represent areas with methane seeps. The western shoreline of the Western Interior Seaway (shaded) is shown during the time of deposition of the *Baculites compressus* Zone. Middle. Close-up showing AMNH localities 3383, 3515, 3528, and 3545. Bottom. Ammonite biostratigraphy of the middle Campanian to lower Maastrichtian, with radiometric dates from Cobban and others (2006), as modified by Landman and others (2018). Seep deposits occur throughout this time interval.

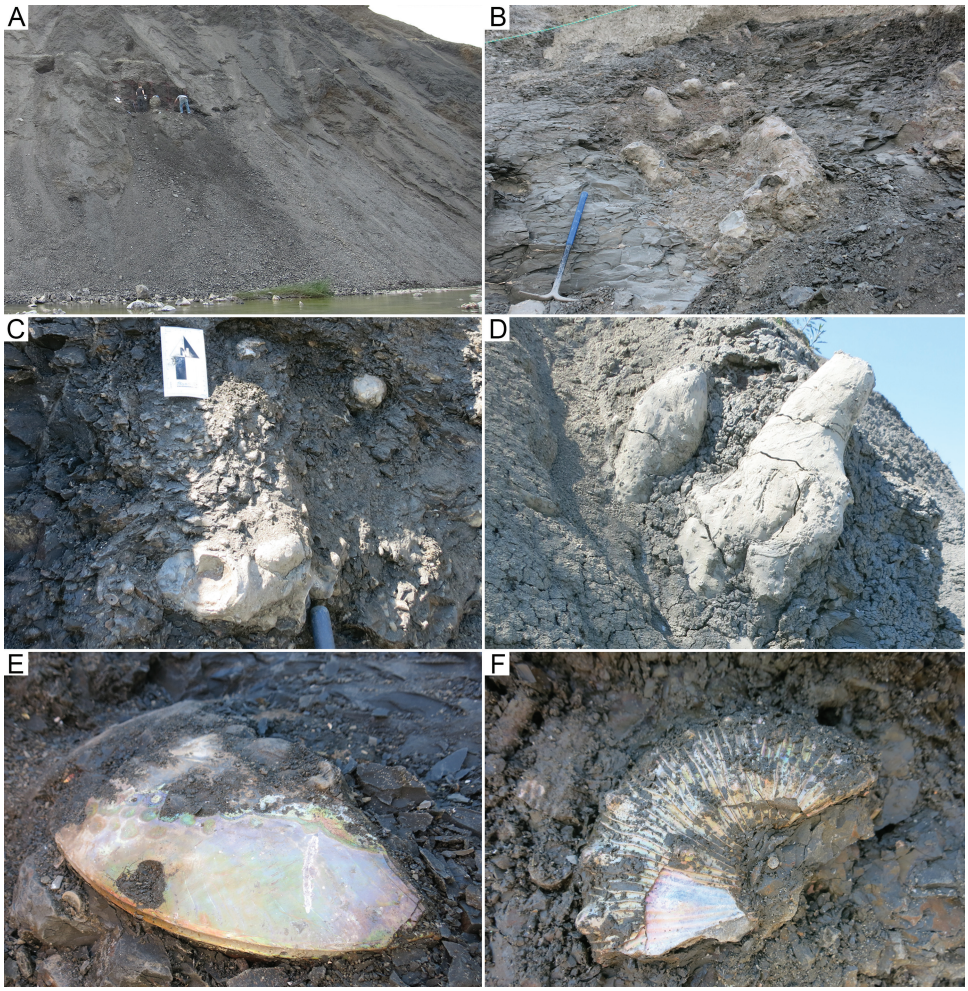

Fig. 2. Methane seep deposits in the *Baculites compressus* Zone, Pierre shale, Meade County, South Dakota. (A) Exposure of seep in cross section revealing the main conduit, AMNH loc. 3528, with people for scale. (B) Close-up of secondary pipes at AMNH loc. 3545. (C, D) Close-ups of seep associated concretions (SAC's), AMNH loc. 3528. (E) *Placenticeras meeki* Böhm, 1898, loose in shale, AMNH loc. 3545. (F) Body chamber of *Hoploscaphites nodosus* (Owen, 1852), loose in shale, AMNH loc. 3545.

which are abundant at both seep and non-seep sites in the Late Cretaceous Western Interior Seaway (WIS).

METHANE SEEP BIOGEOCHEMISTRY

The methane (or hydrocarbon) cold seep environment is characterized by anaerobic oxidation of methane (CH_4), principally via reduction of sulfate (SO_4^{2-}), carried out by a consortium of methanotrophic Archaea and sulfate-reducing bacteria (Iversen and Jørgensen, 1985; Boetius and others, 2000; Campbell, 2006; Alperin and Hoehler, 2009):

$$CH_4 + SO_4^{2-} \rightarrow HCO_3^- + HS^- + H_2O \quad (1)$$

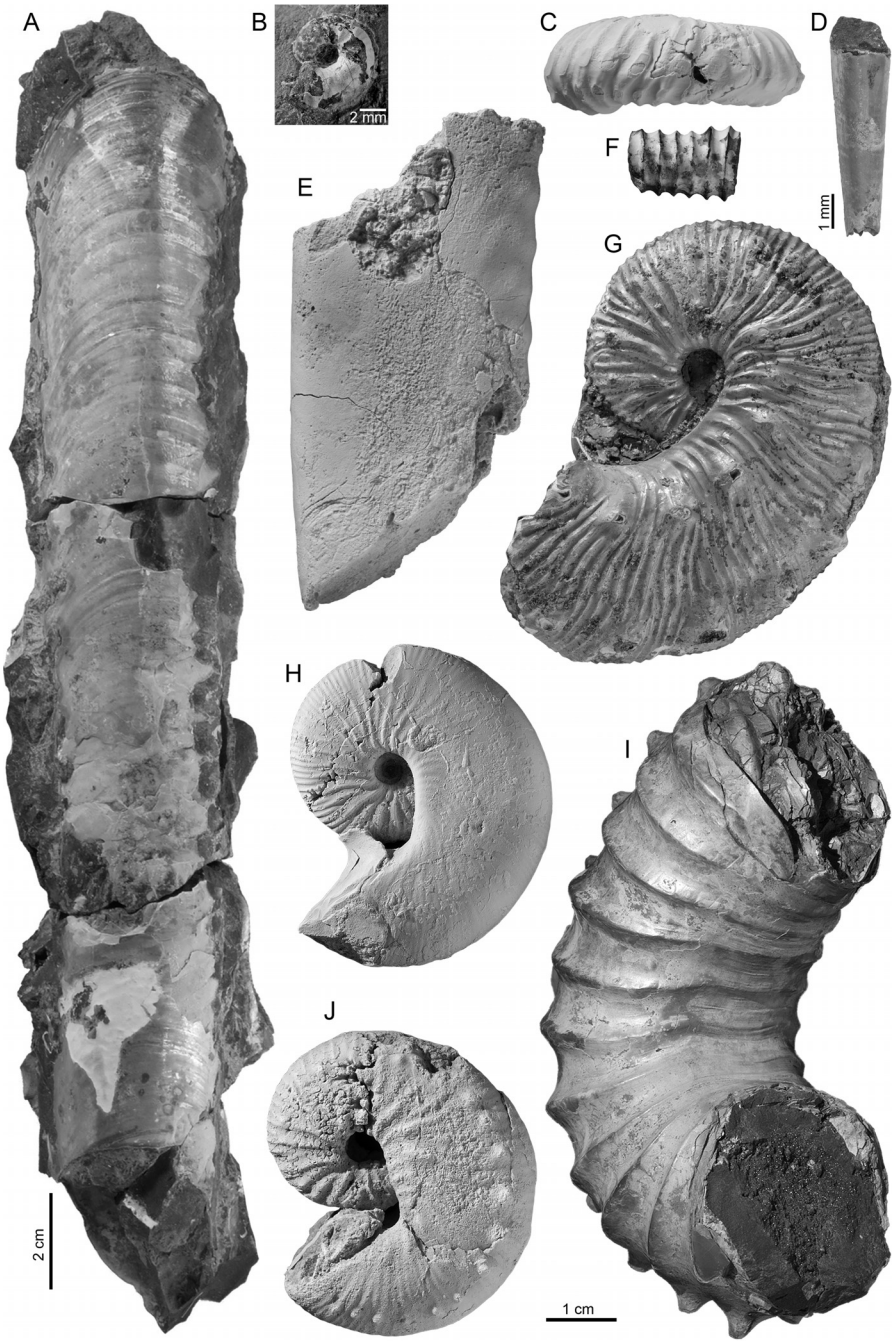

Fig. 3. Ammonite fauna in methane seep deposits in the Campanian Pierre Shale, South Dakota and Wyoming. (A) *Baculites corrugatus* Elias 1933, mature macroconch, ventral view, with aperture on top, AMNH 58552, *Didymoceras cheyennense* Zone. (B) *Hoploscaphites brevis* (Meek 1876), juvenile, left lateral view, AMNH 66244, *Didymoceras cheyennense* Zone. (C) *Didymoceras cheyennense* (Meek and Hayden 1856), fragment, AMNH 63440, *Didymoceras cheyennense* Zone. (D) *Baculites compressus* Say, 1820, juvenile, lateral view, AMNH 112942, *Baculites compressus* Zone. (E) *Baculites compressus* Say 1820, right lateral view, AMNH 58544, *Baculites compressus* Zone. (F) *Spiroxybeloceras meekanum* (Whitfield, 1877), fragment, AMNH 66289, *Didymoceras cheyennense* Zone. (G) *Hoploscaphites brevis* (Meek, 1876), microconch,

TABLE 1

Oxygen and carbon composition of authigenic seep carbonates, Baculites compressus Zone, Pierre Shale, Meade County, South Dakota

Description	Specimen number	AMNH loc.	$\delta^{13}C$ (‰ VPDB)	$\delta^{18}O$ (‰ VPDB)
tube	102525-1	3528	-37.3	-0.9
"	102525-2	3528	-40.5	-0.3
"	102525-4	3528	-39.2	-0.7
"	102525-5	3528	-39.7	-0.6
core	102598	3528	-43.6	-0.6
SAC	102549	3545	-46.1	-0.7
SAC	102577	3545	-47.3	-0.6
SAC	102573	3545	-50.9	-0.8
pipe	102602	3545	-44.7	-0.7
SAC	102588	3545	-45.9	-0.6
SAC	102551	3545	-45.1	-0.6
SAC	102552	3545	-46.9	-0.6
pipe	102553	3545	-43.7	-0.3
pipe	102550	3545	-45.8	-0.5
pipe	102563	3545	-49.8	-0.9

SAC = seep-associated concretion, typically sub-spherical or dumbbell shaped.

The methane produced bacterially (or possibly thermogenically) in organic-rich sediments is enriched in ^{12}C and, as (1) proceeds, the bicarbonate (which dominates the dissolved inorganic carbon (DIC) reservoir) is impressed with very low values of $\delta^{13}C$. Increases in bicarbonate promote the precipitation of calcium carbonate concretions that are imprinted with methane-derived low $\delta^{13}C$ values. Indeed, carbonates from seep sites in the WIS exhibit $\delta^{13}C$ values ranging from ~ -40 permil to ~ -50 permil (Kauffman and others, 1996; Landman and others, 2012; this study, table 1). In addition, analyses of strontium isotopes from seep carbonates in southwestern South Dakota revealed that seep fluids bear signatures that are distinct from the coeval seawater values (Landman and others, 2012; Cochran and others, 2015). Elevation of the $^{87}Sr/^{86}Sr$ in seep fluids likely resulted from exchange with a deep granitic source and suggests that the fluids migrated through the muddy sediments of the Western Interior Seaway.

The diagenetic redox reactions leading to the anaerobic oxidation of methane (AOM) occurred within the sediments over depths to which dissolved sulfate was present–the sulfate-methane transition zone. This was likely relatively close to the sediment-water interface. Previous observations of low $\delta^{13}C$ in ammonite shells from seeps suggested that the pore fluids influenced by AOM must have mixed with the DIC in the overlying water column (Landman and others, 2012). However, the $\delta^{13}C$ of a

Fig. 3 (continued). left lateral view, AMNH 66275, *Didymoceras cheyennense* Zone. (H) *Hoploscaphites gilli* Cobban and Jeletzky 1965, macroconch, left lateral view, USNM 547334, *Baculites scotti–Didymoceras nebrascense* Zones, (non-seep site but also present at age-equivalent seep sites). (I) *Didymoceras cheyennense* (Meek and Hayden 1856), AMNH 102504, *Didymoceras cheyennense* Zone (non-seep site but also present at age-equivalent seep sites). (J) *Hoploscaphites gilberti* Landman and others, 2013, macroconch, left lateral view, AMNH 83717, *Baculites scotti–Didymoceras nebrascense* zones. The 1 cm scale bar on the bottom applies to all specimens except A, B, and D.

mollusc shell is a product of both environmental (that is, DIC) and metabolic effects. Incorporation of respired CO_2 into the shell lowers the $\delta^{13}C$ value of the shell because the respired CO_2 from marine organic matter is enriched in ^{12}C (McConnaughey and Gillikin, 2008). Variable amounts of metabolic carbon incorporated into the shells of different mollusc species can lead to lower $\delta^{13}C$ in some species versus others (Tobin and Ward, 2015). Although some $\delta^{13}C$ values previously measured in seep ammonites are clearly too low to be produced solely by the incorporation of normal marine metabolic carbon (for example, −13.7‰ in a sample of *Didymoceras cheyennense* documented in Landman and others, 2012), the best control is comparison of coeval seep-and non-seep specimens of the same ammonite species, and in the present study we focus on *Baculites compressus*.

LOCALITIES

The seep deposits in this study (AMNH localities 3528 and 3545) are from the upper Campanian *Baculites compressus* Zone of the Pierre Shale in Meade County, southwestern South Dakota (fig. 1, middle). Recent $^{40}Ar/^{39}Ar$ measurements of a bentonite associated with a seep deposit in the *B. compressus* Zone of the Pierre Shale in Custer County, South Dakota, yields an age of 73.79 ± 0.36 Ma (Landman and others, 2018). The seep deposits sampled in this study are newly exposed in cross section along the bluffs of the Cheyenne River (fig. 2A), and are easily recognized because of the presence of large, globular, billowing, bulbous micritic limestone masses as much as several meters in diameter (figs. 2B-2D). These masses co-occur with smaller seep-associated concretions (SAC's; figs. 2 and 2C) consisting of subspherical or dumbbell shaped nodules and pipes, varying from as large as 10 cm in diameter and 40 cm long to small tubes 2 cm in diameter and 10 cm long (Cochran and others, 2015). Fossils are localized and occur in the SAC's as well as in the unconsolidated sediments. The shells are exquisitely preserved, with intact mineralogy and microstructure (figs. 4, 5 and 6). In contrast, the shale immediately surrounding the seep deposits (10's of meters away) is more depauperate. A similar pattern of a concentration of fossils at a seep deposit was documented at another site (AMNH locality 3418) through detailed mapping of the abundance of fossils around the seep by Landman and others (2012).

We also examined specimens at two age-equivalent non-seep sites (AMNH localities 3383 and 3415) in the *Baculites compressus* Zone of the Pierre Shale in Meade and Pennington Counties, South Dakota (fig. 1, middle). These sites are in the same general region as the seep sites (10–50 km away) and have been documented by Fatherree and others (1998) and Landman and Klofak (2012), respectively. These sites are representative of the broad extent of the WIS outside of the seeps. Fossils at these sites are commonly preserved in early diagenetic concretions or loose in the unconsolidated sediments. The concretions vary in shape, size, and fossil content, and usually contain a diverse array of fauna including benthic, nektobenthic, and netktic forms.

All of the localities studied are in southwestern South Dakota (fig. 1, middle) and represent an offshore environment approximately 230 km from the western shoreline of the Seaway (Cobban and others, 1994). However, because no strata of this age are present in eastern Wyoming, the position of the shoreline is difficult to constrain and may have been closer to the studied localities. Indeed, the strata representing the *Baculites compressus* Zone at Red Bird, Wyoming (Gill and Cobban, 1966) are very thin due to non-deposition possibly related to local submarine highs or even emergent areas in the vicinity of the Black Hills at the border between Montana and Wyoming. Recent studies have suggested that most of the Pierre Shale was deposited at a depth of approximately 50 to 100 m during the time of deposition of the *B. compressus* Zone (Landman and others, 2017), although the exact water depth is difficult to establish.

Samples are from the following four localities (fig. 1):

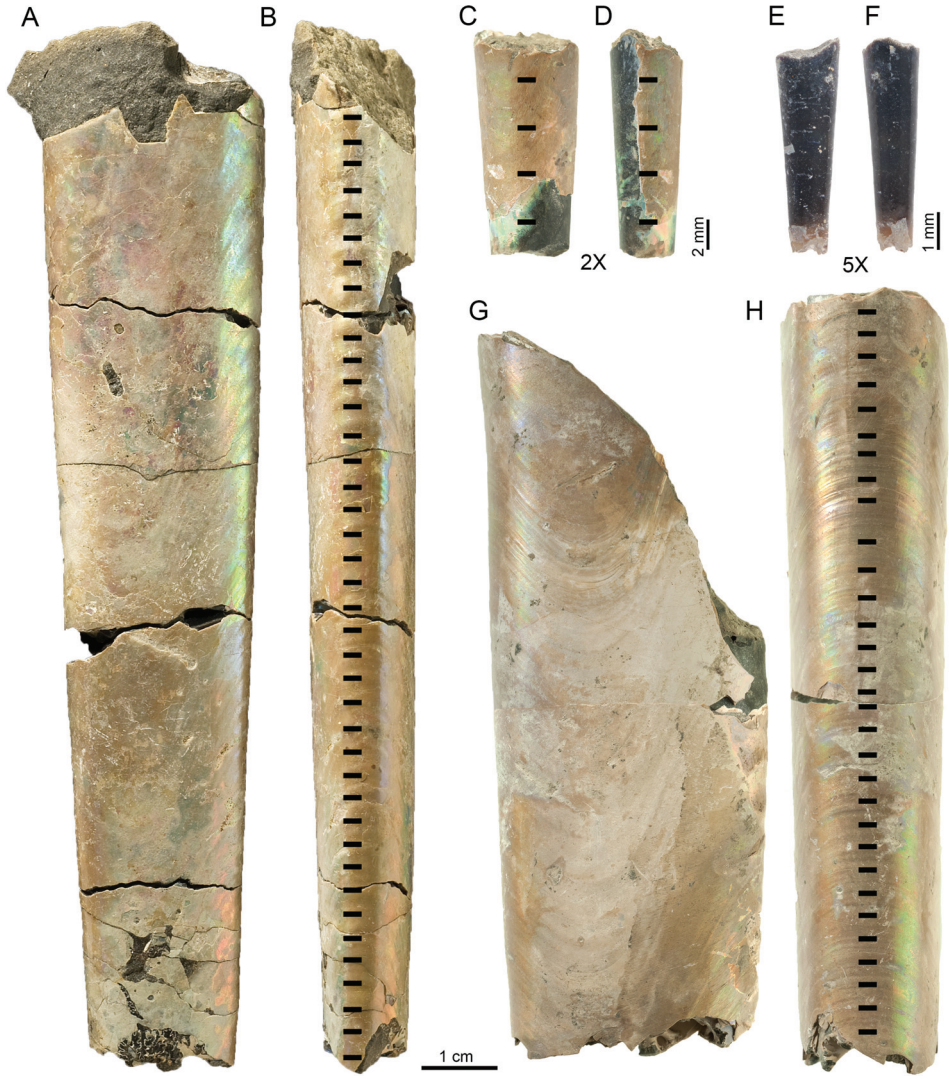

Fig. 4. Specimens of *Baculites compressus* from seep and non-seep sites showing sclerochronological sampling intervals (dashes). (A, B) AMNH 108142, non-seep site, AMNH loc. 3415. A. Right lateral. B. Ventral. (C, D) AMNH 82654, seep site, AMNH loc. 3528. C. Right lateral. D. Dorsal. (E, F) AMNH 112942, seep site, AMNH loc. 3528 (not sampled because of poor preservation). E. Left lateral. F. Dorsal. (G, H) AMNH 64496, seep site, AMNH loc. 3528. G. Right lateral. H. Dorsal. Adoral direction is toward the top.

AMNH loc. 3383, Non-seep deposit, *Baculites compressus* Zone, Pierre Shale, 43.93950 N, −102.83627 W, Pennington County, South Dakota.

AMNH loc. 3415, Non-seep deposit, *Baculites compressus* Zone, Pierre Shale, 44.24125 N, −102.40344 W, Meade County, South Dakota.

AMNH loc. 3528, Methane seep deposit, *Baculites compressus* Zone, Pierre Shale, 44.17306 N, −102.40194 W, Meade County, South Dakota.

AMNH loc. 3545, Methane seep deposit, *Baculites compressus* Zone, Pierre Shale, 44.30972, −102.35056 W, Meade County, South Dakota.

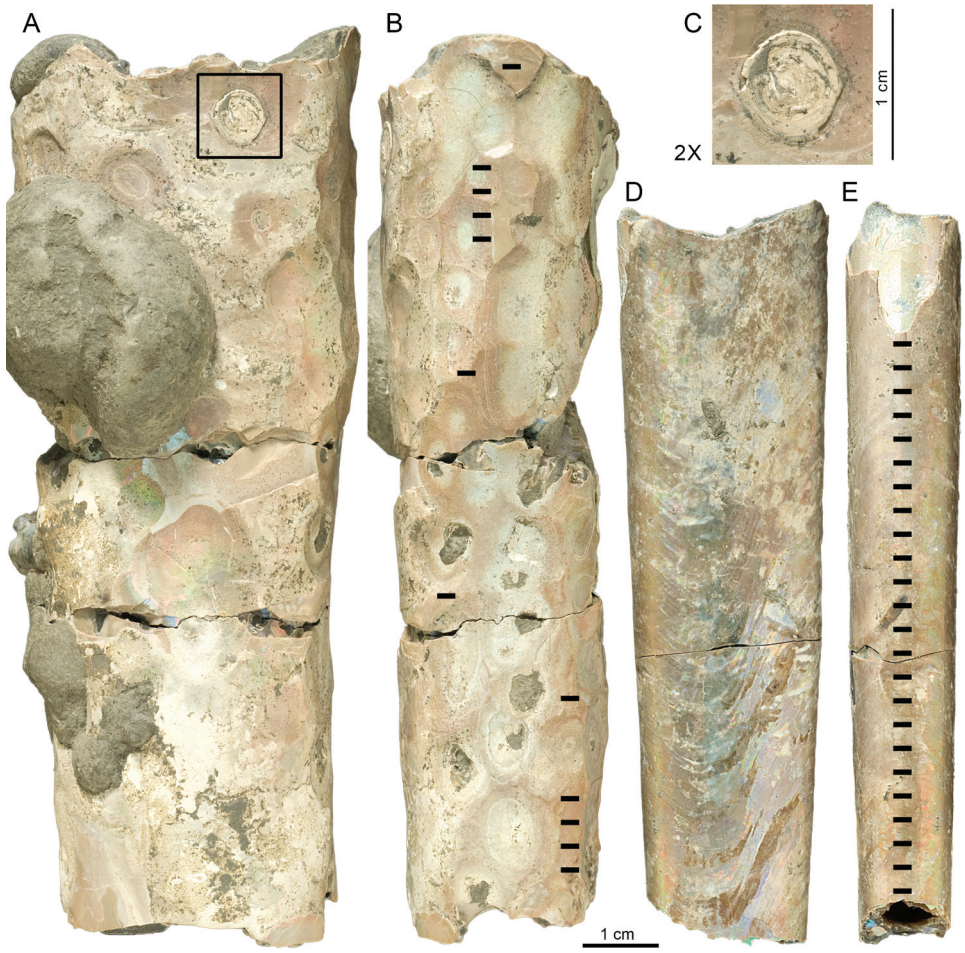

Fig. 5. Specimens of *Baculites compressus* from seep sites showing sclerochronological sampling intervals (dashes). (A, B) AMNH 82656, seep site, AMNH loc. 3258. A. Left side. B. Dorsal. (C) Close-up of limpet on AMNH 82656. (D, E) AMNH 64427, AMNH loc. 3528. D. Right side. E. Dorsal. Adoral direction is toward the top.

MATERIAL

We focused on eight specimens of *Baculites compressus* Say (1820), including the specimen described by Fatherree and others (1998) (figs. 4 and 5). Based on their length, whorl width (WW), and whorl height (WH), they can be sorted into juveniles and possible adults. In this species, as in other Mesozoic ammonites, the adults can be divided into small, slender microconchs and larger, more robust macroconchs (Davis and others, 1996). According to the traditional interpretation, the microconchs are males and the macroconchs are females.

AMNH 64427, AMNH loc. 3528 (seep site), *Baculites compressus*: fragment of body chamber, juvenile, maximum whorl height = 27.2 mm. It was collected loose in the matrix. A total of 23 samples of the outer shell were taken for isotope analysis on the dorsum along the whole length of the shell (98.0 mm). The sampling strategy and sample preparation for this and the other specimens studied are described in the next section.

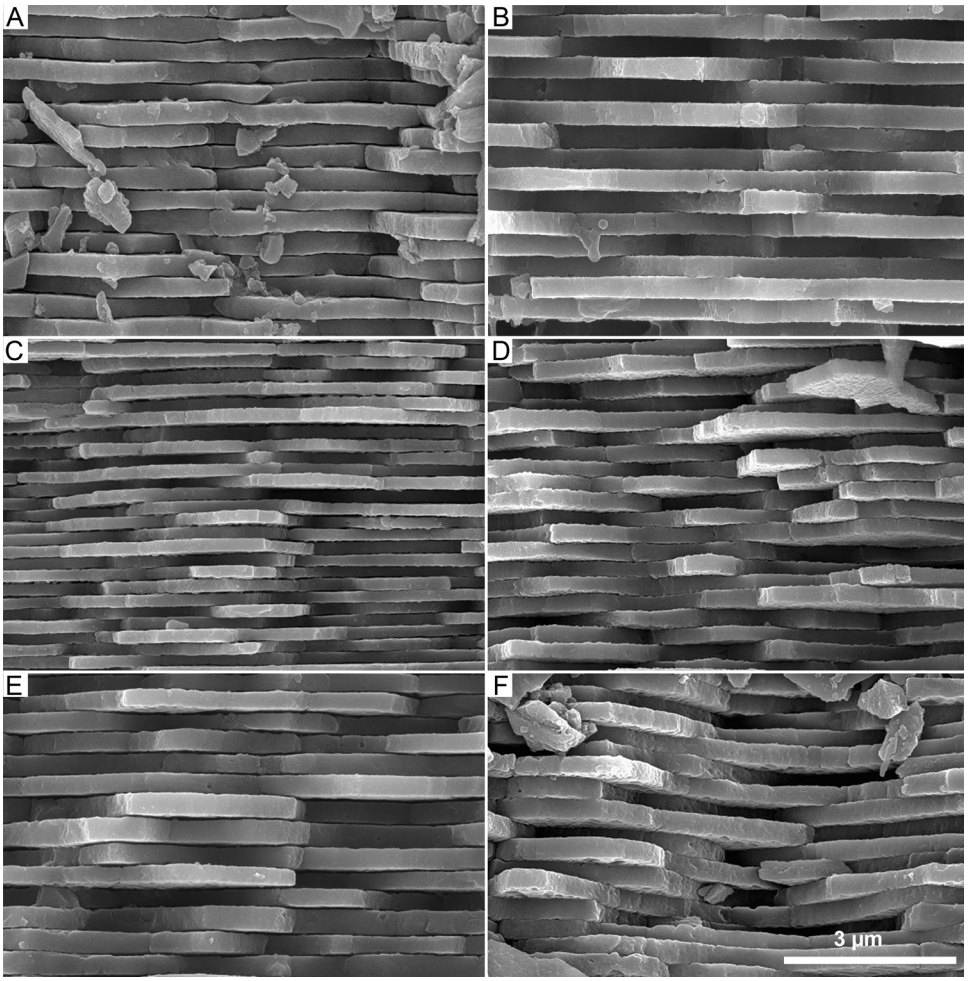

Fig. 6. Representative SEM's of the nacreous microstructure of *Baculites compressus* analyzed for isotopes. The shell samples show excellent preservation, with Preservation Index = 4–5 (Cochran and others, 2010). (A) AMNH 108142, non-seep site, AMNH loc. 3415. (B) AMNH 64427, seep site, AMNH loc. 3528. (C) AMNH 82654, seep site, AMNH loc. 3528. (D) AMNH 65596, seep site, AMNH loc. 3528. (E) AMNH 82655, seep site, AMNH loc. 3528. (F) AMNH 64526, seep site, AMNH loc. 3545.

AMNH 64496, AMNH loc. 3528 (seep site), *Baculites compressus*: fragment of the adapical part of the body chamber, adult (microconch?), maximum whorl height = 36.6 mm. One-half of the ventral part of the body chamber is broken off, consistent with damage from predation. It was collected loose in the matrix. A total of 31 samples of the outer shell were taken for isotope analysis on the dorsum along the whole length of the shell (93.5 mm).

AMNH 64526, AMNH loc. 3545 (seep site), *Baculites compressus*: fragment of body chamber, adult (macroconch), maximum whorl height = 56.8 mm. It was collected loose in the sediment. A total of 46 samples of the outer shell were taken for isotope analysis on the dorsum along the whole length of the shell (139.0 mm).

AMNH 66330, AMNH loc. 3383 (non-seep site), *Baculites compressus*: 280 mm in length, 170 mm of which is phragmocone, probably a macroconch, maximum whorl

height = 57.2 mm. This specimen was studied by Fatherree and others (1998) who analyzed 38 samples of the outer shell on the ventral part of the flanks along the entire length of the specimen. They assigned the specimen to *B. compressus*, but Palamarczuk and Landman (2011) noted that the specimen is very compressed with a somewhat tabulate venter and speculated that it could represent a closely related species from a slightly younger interval, but still within the middle upper Campanian. For purposes of the present study, we consider it as comparable to the non-seep specimen of *B. compressus* analyzed by us (AMNH 108142).

AMNH 82654, AMNH loc. 3528 (seep site), *Baculites compressus*: fragment of a body chamber, juvenile, maximum whorl height = 6.5 mm. A total of 4 samples of the outer shell were taken for isotope analysis on the flanks along the whole length of the shell (14.9 mm).

AMNH 82655, AMNH loc. 3528 (seep site), *Baculites compressus*: most of the phragmocone and part of the body chamber, adult macroconch, maximum whorl height = 69.4 mm. This specimen provides the longest ontogenetic record. It was collected loose in the matrix. Parts of the shell are missing on both sides. The specimen exhibits a few limpet home scars. A total of 26 samples of the outer shell were taken for isotope analysis along the whole length of the shell (600–700 mm), mostly on the dorsal part of the flanks, except for three samples on the ventral part of the flanks, but not in an adjacent area.

AMNH 82656, AMNH loc. 3528 (seep site), *Baculites compressus*: fragment of the adoral part of the body chamber, adult (macroconch?), maximum whorl height = 48.2 mm. It was collected loose in the matrix. The adoral part of the right side of the shell is missing. The whole specimen is covered with limpet home scars. A total of 9 samples of the outer shell were taken for isotope analysis on the dorsum along the whole length of the shell (122 mm).

AMNH 108142, AMNH loc. 3415 (non-seep site), *Baculites compressus*: adoral part of the phragmocone and a small portion of the body chamber, large juvenile to adult, possibly microconch, maximum whorl height = 29.8 mm. The adoral edge of the shell is broken and forms sharp re-entrants, consistent with predatory damage (Takeda and others, 2015). It was collected loose in the matrix. A total of 40 samples of the outer shell were taken for isotope analysis on the venter along the whole length of the shell (129.3 mm).

We also sampled pieces of carbonate matrix from two seep sites. We analyzed five samples from AMNH loc. 3528 consisting of tubes and massive micritic limestone and 10 samples from AMNH loc. 3545 consisting of pipes and SAC's. The carbonate content of seep-associated concretions from these sites is 85 to 89 percent by weight.

SHELL MICROSTRUCTURE AND ISOTOPE ANALYSIS

All shell samples were visually inspected to determine the state of preservation, and only samples whose shell material appeared unaltered were chosen for analysis. Prior work has shown that the state of preservation of nacreous shell microstructure of aragonitic ammonite shells is an excellent predictor of the integrity of their O, C and Sr isotope signatures (Cochran and others, 2003, 2010; Knoll and others, 2016). Accordingly, scanning electron microscope (SEM) analysis was undertaken to determine the degree of alteration of each sample. Sample preservation was in general very good (Preservation Index = 3) to excellent (Preservation Index = 5), according to the Preservation Index (PI) scale of Cochran and others (2010). This scale is based on the preservation of the nacreous microstructure characteristic of ammonite shells (and other molluscs). As preservation degrades, the nacreous tablets fuse together, eventually becoming virtually indistinguishable (PI = 1, poor preservation). However, even at this stage of preservation, the carbonate remains fundamentally aragonite, and Cochran and others (2010) have discussed the mechanisms responsible. Examples of

preservation of the samples studied are shown in figure 6. The PI values of every sample are listed in tables A1-A7.

In most specimens, samples were taken every 3 mm continuously on the venter, dorsum, or flanks along the longest continuous unbroken stretches of shell. Each sample site was constrained to a length of 3 mm parallel to the axis of shell growth with 1 to 2 mm on either side, depending on the amount of material available in order to accumulate enough mass for analysis. At any given sample site, the topmost layer of shell was removed with deionized water and mechanical preparation to eliminate any remnants of attached shale or concretion matrix. Then a square was inscribed into the shell and more deionized water was applied. A flat blade was pressed to the side of the sample square so that the shell fragments did not fly off. Deionized water was used to pick up shell pieces and subdivide them into two plastic vials, one for isotope analysis and one for assessment with SEM. Figures 4 and 5 indicate the positions of samples on each specimen. Whorl heights were measured by digital calipers to the nearest 0.1 mm at the positions where samples were taken for isotope measurement and SEM imaging.

Shell pieces were mounted on SEM stubs in two orientations showing the surface and cross section of the shell. Samples were coated with gold, and then analyzed using a Hitachi S-4700 Field Emission SEM. Samples were viewed under 15kV with an aperture at 20μm using a secondary electron detector. The shell surfaces were viewed and photographed at 2000X and shell cross sections were viewed and photographed at 5000 and 15000X. The state of preservation of each sample was scored according to the Preservation Index of Cochran and others (2010). The SEM preservation index ranged from 2.5 to 4.5 (fig. 6). We only included samples with PI $\geq$ 3 in our study to assure that, in principle, the shell material preserved the original isotope signature. In AMNH 66330, the state of preservation was evaluated by Fatherree and others (1998) who noted "unaltered" nacreous tablets but did not assign a PI value. Based on their illustration, the PI =4 (Fatherree and others, 1998, fig. 3).

The $\delta^{13}C$ and $\delta^{18}O$ values of the samples were determined at the University of California, Santa Cruz, Stable Isotope Laboratory (UCSC SIL). Prior to analysis, 40 to 60 micrograms of solid sample were vacuum-roasted overnight to remove any residual organic material occurring between the nacreous tablets. Samples were analyzed for $\delta^{18}O$ and $\delta^{13}C$ via acid digestion using an individual vial acid drop ThermoScientific Kiel IV carbonate device interfaced to a ThermoScientific MAT-253 dual-inlet isotope ratio mass spectrometer (IRMS). Samples were reacted at 75 °C in orthophosphoric acid (specific gravity = 1.92 g/cm^3) to generate carbon dioxide and water. Non-condensable gases were pumped away and the CO_2 analyte was then cryogenically separated from water, finishing with the introduction of pure CO_2 into the IRMS via the dual inlet.

Raw data were corrected using a two-point calibration against samples of calibrated in-house granular Carrara Marble standard reference material ($\delta^{13}C = 2.05 \pm 0.1‰$ and $\delta^{18}O = -1.91 \pm 0.1‰$ VPDB) and granular NBS-18 limestone international standard reference material. The in-house Carrara Marble was extensively calibrated against NIST Standard Reference Material (NBS-19, NBS-18, and LSVEC) and further calibrated in intercomparison studies with international laboratories. Raw data were corrected for offset from the international standard PDB (PeeDee Belemnite) for $\delta^{18}O$ and $\delta^{13}C$ and corrected for instrument-specific source ionization effects. Aliquots of an external working standard (powdered Atlantis II calcium carbonate; $\delta^{18}O = 3.42‰$) were run "as-a-sample" to monitor quality control and long-term performance. Typical precision is 0.05 permil (1σ) for both $\delta^{18}O$ and $\delta^{13}C$. All values are reported relative to VPDB.

We converted the values of $\delta^{18}O$ to temperature using the equation of Grossman and Ku (1986) for molluscan aragonite, as modified by Hudson and Anderson (1989) such that the δ_{water} values are corrected for the difference between PDB and SMOW:

$$T(°C) = 19.7 - 4.34(\delta_{aragonite} - \delta_{water}) \quad (2)$$

We assumed that the $\delta^{18}O_{water}$ of the Late Cretaceous Western Interior Seaway was −1 permil (Shackleton and Kennett, 1975) and that the salinity was typical of normal marine values. The value of −1 permil agrees with estimates based on studies of clumped isotopes by Dennis and others (2013) of −1.2 ± 0.2 permil VSMOW for the *Baculites compressus* Zone in South Dakota. Petersen and others (2016) also used clumped isotopes to determine $\delta^{18}O_{water}$ for offshore WIS sites typical of the settings in the present study and calculated values ranging from −1 permil to −4 permil. The two studies differ fundamentally in that Dennis and others (2013) focused on ammonites while Petersen and others (2016) analyzed bivalves and gastropods. As well, the value from Dennis and others (2013) cited above is solely based on isotope analyses of ammonites in the *B. compressus* Zone, while Petersen and others (2016) combined samples spanning several million years during the Late Cretaceous. Our purpose here is not to reconstruct salinity or temperature distributions in the WIS, but rather to compare seep and non-seep *B. compressus* from a relatively restricted area of the WIS during the time of deposition of the *B. compressus* Zone. Accordingly, we use $\delta^{18}O_{water} = -1$ permil.

RESULTS

The samples of authigenic carbonates (all Mg-calcite) from the two seep sites reveal very low values of $\delta^{13}C$ (table 1). In AMNH loc. 3528, the values range from −43.6 permil to −37.3 permil. In AMNH loc. 3545, the values are slightly lower, ranging from −50.9 permil to −43.6 permil. Values of $\delta^{18}O$ are nearly the same in both localities and range from −0.9 permil to −0.3 permil.

The results of C and O isotope analyses of the specimens of *Baculites compressus* are summarized in figures 7, 8 and 9 and tables 2 and 3 and presented fully in the Appendix (tables A1-A7; all values are reported relative to VPDB; averages are reported ± 1 standard deviation). The specimens overlap in size, allowing us to determine if a correlation exists between shell size and isotope composition. To facilitate comparisons of the isotope values of specimens with different sizes, we plotted the values as a function of whorl height (figs. 7 and 8). As the specimen grew, the whorl height increased, so the sclerochronological plots are effectively a function of time through ontogeny. However, the time interval between successive samples in any individual is not necessarily constant.

Each of the specimens was sampled along the growth axis. Because of limitations imposed by availability of shell material, we sampled along the dorsum in AMNH 64427, 64496, 64526, and 82656, along the venter in AMNH 108142, and on the flanks in AMNH 82655 and 82654. In AMNH 82655, we obtained 26 samples from the dorsal part of the flanks and 3 samples from the ventral part of the flanks. However, the sequences of samples on the two parts of the flanks are not adjacent, precluding the possibility that we inadvertently sampled along a single growth line. Fatherree and others (1998, figs. 2C and 5A) noted variation in the isotope composition of shell material from different parts of the shell wall in a single specimen, even along what was presumably a single growth line. They could not completely explain this variation although they attributed it to differences in shell thickness and concomitant differences in the amount of time averaging. They reported a range of $\delta^{13}C$ of as much as 0.3 and 0.4 permil on an adapical and adoral growth line, respectively (omitting a single anomalous point in the analysis of each growth line). This difference

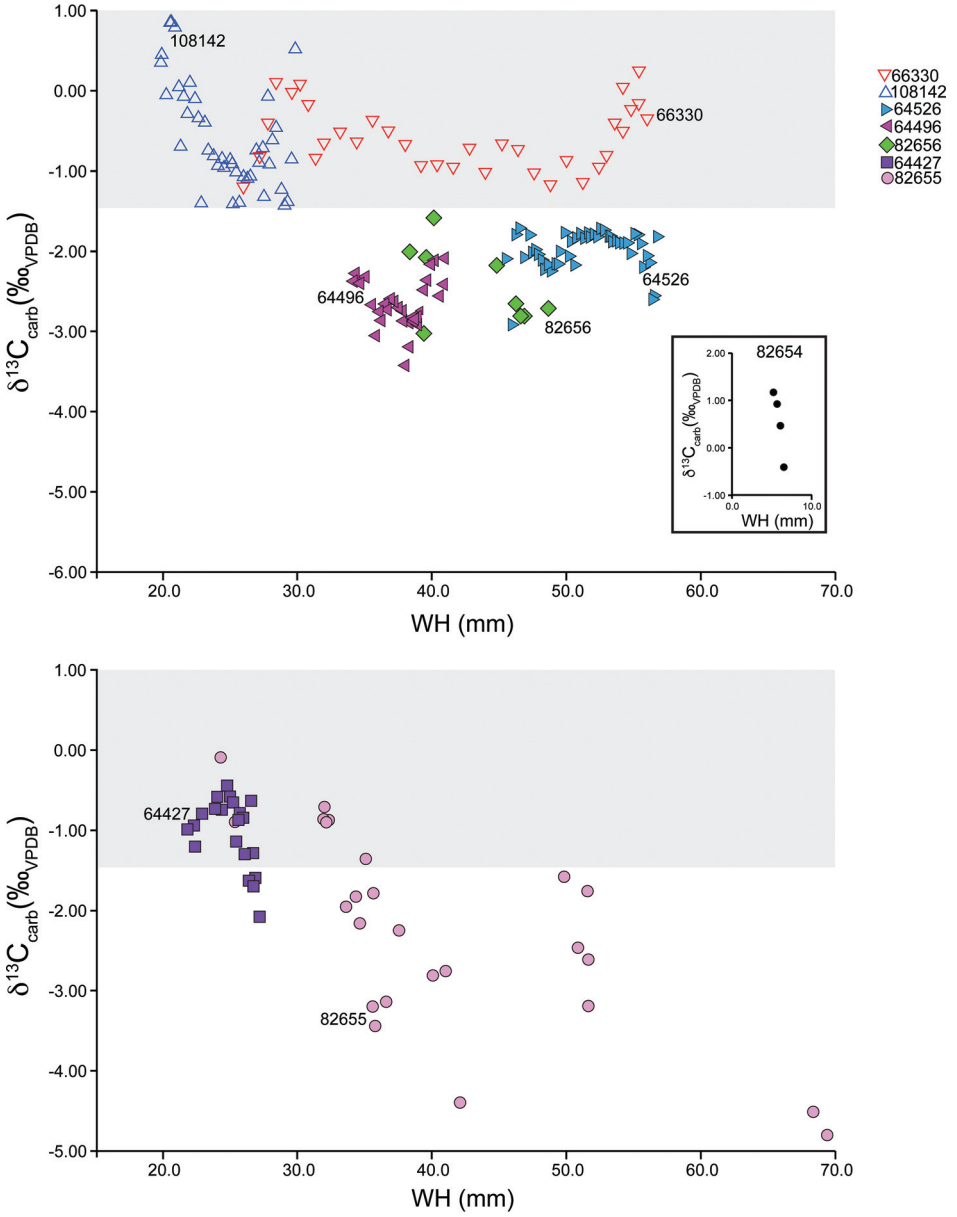

Fig. 7. Comparison of $\delta^{13}C$ values (in ‰ VPDB) of *Baculites compressus* from both seep and non-seep sites plotted against whorl height (WH). (A) Comparison of seep and non-seep specimens. The gray area demarcates the isotope values characteristic of the non-seep environment. Solid symbols are seep specimens; open symbols are non-seep specimens. (B) Seep specimens in which the values of $\delta^{13}C$ in early ontogeny suggest that the animals lived in a non-seep environment (gray area) but migrated into a seep environment as ontogeny progressed. See table 3 for statistical comparison of data.

is less than that between seep and non-seep environments, as reported below. Therefore, the position of the samples on the shell (dorsum versus venter versus flanks) is unlikely to affect our interpretation.

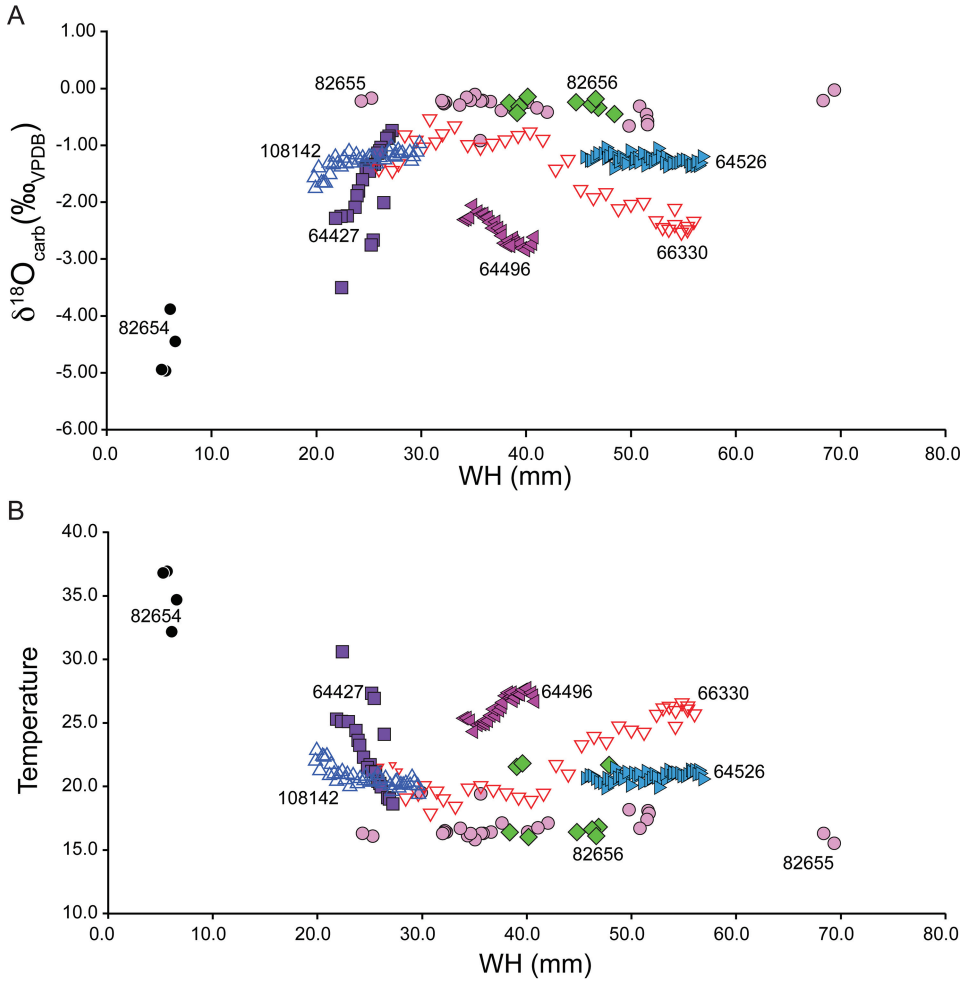

Fig. 8. (A) Comparison of $\delta^{18}O$ values (in ‰ VPDB) of *Baculites compressus* from both seep and non-seep environments against whorl height (WH). Solid symbols are seep specimens; open symbols are non-seep specimens.

The isotope values of the shell samples from the non-seep sites show a weak cyclic pattern (fig. 7A). In AMNH 66330, an adult macroconch, which was analyzed by Fatherree and others (1998), the values of $\delta^{13}C$ are high in early ontogeny, low in middle ontogeny, and high again at the end of ontogeny. They average -0.6 ± 0.4 permil and range from -1.2 to 0.1 permil. The values of $\delta^{18}O$, on the other hand, are relatively constant in early ontogeny and decrease steadily to low values in later ontogeny. They average -1.6 ± 0.7 permil and range from -2.6 permil to -0.6 permil. The calculated temperatures average 22 ± 3 °C and range from 18 °C to 27 °C. In AMNH 108142, a late juvenile or adult microconch, the values of $\delta^{13}C$ are high in early ontogeny, low in middle ontogeny, and high again in later ontogeny. They average -0.6 ± 0.7 permil and range from -1.4 permil to 0.9 permil. The values of $\delta^{18}O$, on the other hand, show a steady increase to higher values throughout the sampled interval. They average -1.3 ± 0.2 permil and range from -1.8 permil to -1.0 permil. The calculated temperatures average 21 ± 1 °C and range from 20 °C to 23 °C.

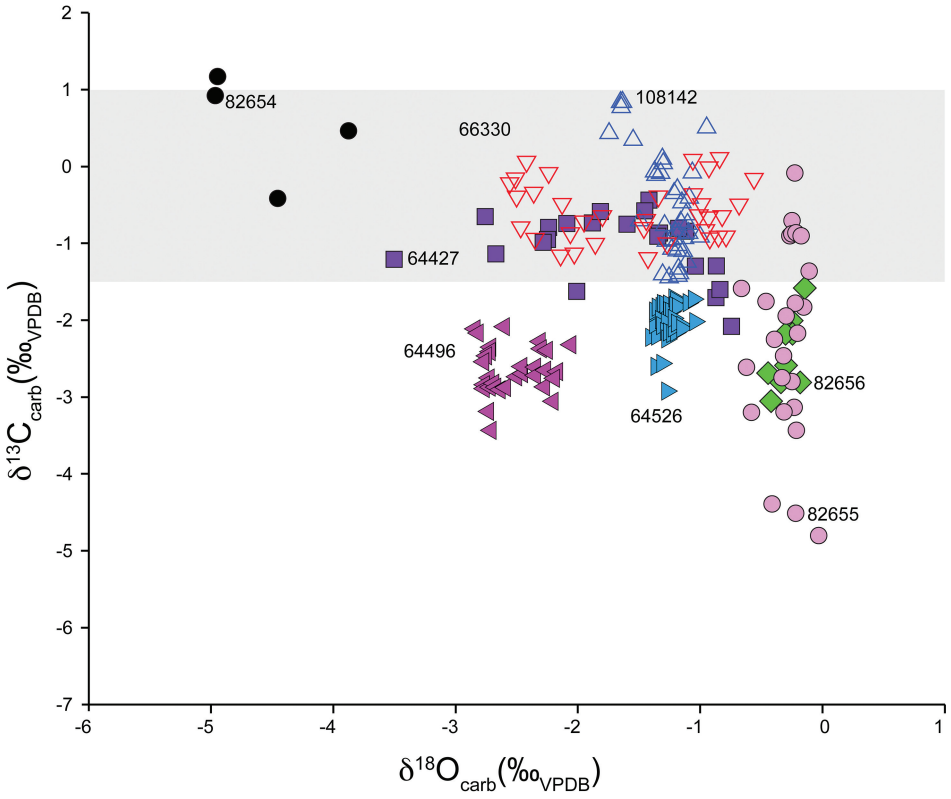

Fig. 9. Cross-plot of $\delta^{13}C$ vs $\delta^{18}O$ (all in ‰ VPDB) in seep (solid symbols) and non-seep (open symbols) of *Baculites compressus* from localities analyzed in this study. The gray area demarcates isotope values characteristic of the non-seep environment. See Appendix 1 for data.

The specimens from the seep localities show three isotope patterns, the first of which consists of nearly constant values (figs. 7A and 8). In AMNH 64526, the body chamber of a mature macroconch, the values of $\delta^{13}C$ average -2.0 ± 0.3 permil and range from -2.9 permil to -1.7 permil. The values of $\delta^{18}O$ average -1.3 ± 0.1 permil and range from -1.4 permil to -1.0 permil. The calculated temperatures average $21° \pm 0.4$ °C and range from 20 °C to 21 °C. In AMNH 64496, the values of $\delta^{13}C$ average -2.7 ± 0.3 permil and range from -3.4 permil to -2.1 permil. The values of $\delta^{18}O$ average -2.5 ± 0.2 permil and range from -2.8 permil to -2.1 permil. The calculated temperatures average 26 ± 1 °C and range from 24 °C to 28 °C. In AMNH 82656, which is a phragmocone of a large macroconch, the values of $\delta^{13}C$ average -2.5 ± 0.5 permil and range from -3.1 permil to -1.6 permil; values of $\delta^{18}O$ average -0.3 ± 0.1 permil and range from -0.5 permil to -0.2 permil. The calculated temperatures average 17 ± 0.5 °C and range from 16 °C to 17 °C.

Two other specimens from seep localities show trends in isotope values with whorl height (figs. 7 and 8). In AMNH 64427, a large juvenile, the values of $\delta^{13}C$ are relatively stable and high in early ontogeny and then decline beginning at WH = 25.2 mm. They average -0.8 ± 0.2 permil in early ontogeny and -1.6 ± 0.3 permil in later ontogeny. In contrast, the values of $\delta^{18}O$ increase throughout ontogeny, with some notable reversals. They average -1.9 ± 0.7 permil in early ontogeny and -1.1 ± 0.5 permil in later ontogeny. The calculated temperatures average $24 \pm 3°$ and 20 ± 2 °C,

TABLE 2

Averages (± 1 standard deviation) of carbon and oxygen isotope values and calculated water temperatures for Baculites compressus from seep and non-seep sites, B. compressus Zone, Pierre Shale, Meade County, South Dakota

Specimen no.	Seep/non-seep	AMNH loc.	n	$\delta^{13}C$ (‰VPDB)	$\delta^{18}O$ (‰ VPDB)	Temperature (°C)
Collected at seep sites						
64526	Seep	3545	46	-2.0 ± 0.3	-1.3 ± 0.1	21 ± 0.4
64496	Seep	3528	31	-2.7 ± 0.3	-2.5 ± 0.2	26 ± 1
82656	Seep	3528	9	-2.5 ± 0.5	-0.3 ± 0.1	17 ± 0.5
64427	Non-seep*	3528	16	-0.8 ± 0.2	-1.9 ± 0.7	24 ± 3
	Seep**	"	6	-1.6 ± 0.3	-1.1 ± 0.5	20 ± 2
82655	Non-seep*	3528	6	-0.7 ± 0.3	-0.2 ± 0.03	16 ± 0.1
	Seep**	"	16	-2.7 ± 1.0	-0.3 ± 0.2	17 ± 0.7
82654	Seep	3528	4	0.5 ± 0.7	-4.6 ± 0.5	35 ± 2
Collected at non-seep sites						
108142		3415	40	-0.6 ± 0.7	-1.3 ± 0.2	21 ± 1
66330^		3383	34	-0.6 ± 0.3	-1.6 ± 0.7	22 ± 3

^ = Fatherree and others (1998); * = inferred non-seep portion of the sclerochronological record; ** = inferred seep portion of the record.

respectively. In AMNH 82655, a large macroconch, the values of $\delta^{13}C$ show a steady decline with a few notable reversals. The values of $\delta^{13}C$ average -0.7 ± 0.3 permil in early ontogeny and -2.7 ± 1.0 permil in later ontogeny. The values of oxygen are nearly constant, averaging -0.2 ± 0.03 permil in early ontogeny and -0.3 ± 0.2 permil in later ontogeny. The calculated temperatures average 16 ± 0.1 °C and 17 ± 0.7 °C, respectively.

The single small juvenile collected at a seep locality (AMNH 82654) shows some of the highest values of carbon and the lowest values of oxygen observed in this study. The values of $\delta^{13}C$ average 0.5 ± 0.7 permil and range from -0.4 to 1.2 permil. The values of $\delta^{18}O$ average -4.6 ± 0.5 permil and range from -5.0 to -3.9 permil. The calculated temperatures average 35 ± 2 °C and range from 32° to 37 °C.

TABLE 3

Results of unpaired t-tests comparing average $\delta^{13}C$ values of Baculites compressus from seep and non-seep sites, B. compressus Zone, Pierre Shale, Meade County, South Dakota

Seep specimen	vs	Non-seep specimen	t-test result
64526		108142	$p < 0.0001$ (VVS)
64496		108142	$p < 0.0001$ (VVS)
82656		108142	$p < 0.0001$ (VVS)
64427: non-seep portion		108142	NS
64427: seep portion		108142	$p < 0.0001$ (VVS)
82655: non-seep portion		108142	NS
82655: seep portion		108142	$p < 0.0001$ (VVS)

VVS = difference is extremely significant; NS = difference is not significant.

DISCUSSION

Methane Seeps as Ammonite Habitats: Evidence from C and O Isotopes

The values of $\delta^{13}C$ in the authigenic Mg-calcite of the seep carbonate concretions are very low, ranging to as low as ~ −51 permil. These values are comparable to those reported from other seep deposits in the Upper Cretaceous Western Interior (Kauffman and others, 1996; Landman and others, 2012). They stand in contrast to the carbonate cement in non-seep fossiliferous concretions from the WIS. Landman and Klofak (2012) reported $\delta^{13}C$ values higher than −22 permil in a concretion from the *Baculites compressus* Zone and Landman others (2015) reported values of higher than ~ −16 permil in a concretion from the higher *Baculites baculus* Zone (Landman and others, 2015). These differences between seep and non-seep concretions indicate that the very low values observed in the SAC's were produced by the anaerobic oxidation of methane, as observed in both modern and ancient methane seep deposits (Peckmann and Thiel, 2004).

The two specimens of *Baculites compressus* from non-seep sites comprise the range of values of $\delta^{13}C$ characteristic of these settings (shown highlighted in gray in figs. 7A and 7B), with values in the two specimens spanning the range from 0.9 permil to −1.4 permil (fig. 7A). Previous measurements of $\delta^{13}C$ in well-preserved specimens of *B. compressus* from non-seep sites by Cochran and others (2010), Landman and Klofak (2012), and Dennis and others (2013) show similar values, with an average of -1.2 ± 0.8 permil ($n = 16$).

In contrast, the seep specimens show lower values of $\delta^{13}C$ in all or part of their ontogeny (figs. 7A and 7B). Three of the specimens show $\delta^{13}C$ values that are lower than those for non-seep specimens throughout the portions of the shells sampled (fig. 7A). The mean $\delta^{13}C$ values in these three specimens are extremely significantly different ($p < 0.0001$) from those of the non-seep specimen AMNH 108142 based on an unpaired t-test (table 3). A t-test was chosen for comparison of seep and non-seep mean $\delta^{13}C$ values because sample sizes are relatively large, and based on the central limit theorem, the mean of a large sample is approximately normally distributed.

Two other specimens collected at seep site AMNH loc. 3528 show a combination of non-seep and seep signatures (fig. 7B). In AMNH 64427, a large juvenile, the values of $\delta^{13}C$ are relatively high in early ontogeny and then decline beginning at WH = 25.2 mm. Compared with non-seep specimen AMNH 108142, the mean values in early ontogeny are not significantly different versus those in later ontogeny, which are significantly different ($p < 0.0001$; table 3). If the values of $\delta^{13}C$ recorded in the non-seep specimens are used as a guide, it implies that this animal must have migrated to the seep environment in later ontogeny. Similarly, in AMNH 82655, which is a large macroconch, the values of $\delta^{13}C$ depart from the non-seep field at WH ~34 mm and remain below it, attaining −4 to −5 permil by WH = 69 mm. Compared with the non-seep specimen AMNH 108142, the mean values in early ontogeny are not significantly different, but those in later ontogeny are significantly different ($p < 0.0001$; table 3). This similarly implies that the animal arrived at the seep as a late juvenile and remained there the rest of its life.

AMNH 82654 is a small juvenile less than 7 mm whorl height, with only four samples. This specimen shows a different isotope pattern from all the other specimens, with some of the highest values of $\delta^{13}C$ and the lowest values of $\delta^{18}O$ observed in this study (fig. 7A, insert; figs. 8 and 9). The values of $\delta^{13}C$ range from −0.4 to 1.2 permil and the values of $\delta^{18}O$ range from −5.0 to −3.9 permil. The calculated water temperature averages 35 °C approaching the temperature tolerance limit of modern cephalopods. Although the exact temperature and salinity requirements of ammonites are unknown, modern cephalopods cannot tolerate salinities below approximately 20 (PSU) nor temperatures above 35 °C (Vidal and others, 2014). Thus, although this

specimen was collected at a seep site, it apparently did not live there. Taken together, the $\delta^{13}C$, $\delta^{18}O$, and calculated temperatures suggest that the juvenile secreted its shell in the upper water column, where temperatures were higher, the salinity was possibly reduced (Petersen and others, 2016), and the value of $\delta^{13}C$ of the DIC was higher, as in the modern ocean and as reconstructed for the Late Cretaceous proto-Gulf Coast (Sessa and others, 2015; see further discussion below).

Linzmeier and others (2018) have used SIMS analyses to elucidate the early ontogenetic stages of *Hoploscaphites*, another ammonite that inhabited the Western Interior Seaway. They argued that these ammonites spent time in the near-surface water column in their early ontogeny, likely as a component of the plankton. The juvenile specimen of *Baculites compressus* analyzed in the present study was found at a seep, so the animal must have died there soon after arriving. Interestingly, Rowe and others (2017, 2018) and Landman and others (2012, fig. 3K) reported many small juveniles of *Baculites* and *Hoploscaphites* at seep sites in the WIS. Our isotope results suggest that these individuals arrived at the seeps early in ontogeny, and died there either because of predation or, possibly, suffocation due to the toxic effects of hydrogen sulfide (H_2S), which was produced during the anaerobic oxidation of methane (Boetius and others, 2000). The introduction of seep fluids to the overlying water, as documented in the present study and by Landman and others (2010) and Cochran and others (2015), suggests that H_2S concentrations may have been elevated in the overlying water, particularly close to the sediment-water interface. This could have had a disproportional effect on newly arrived juveniles of *Baculites*, which were more vulnerable than larger specimens.

A plot of $\delta^{13}C$ as a function of whorl height permits a comparison of isotope composition versus shell size. In the two seep specimens that include samples with WH <30 mm (AMNH 64427 and 82655), the values of $\delta^{13}C$ for that size range plot in the field defined by the non-seep specimens (fig. 7B). At WH >30 mm, the values of $\delta^{13}C$ of all of the seep specimens (AMNH 64496, 82656, 64526, and 82655) are significantly lower than those in non-seep specimens. Thus, the only detectable trend with size in seep specimens is toward lower values with larger size. In fact, if AMNH 64496, 82656, and 64526 were more complete, including early ontogeny, they may have shown the same trend.

In contrast to the $\delta^{13}C$ results, values of $\delta^{18}O$ show no consistent offset between seep and non-seep specimens (fig. 8A). In terms of $\delta^{18}O$ and the calculated water temperatures from equation 1, the specimens of *Baculites compressus* from the seep and non-seep sites are closely similar, with the exception of the small juvenile (figs. 8A and 8B). The small juvenile displays unusually warm temperatures, and as noted above, likely spent this portion of its life in warmer, lower salinity surface waters, as envisioned by Petersen and others (2016). The averages of the calculated temperatures of the other specimens range from 16 to 24 °C (table 2). In general, these values are quite characteristic of WIS temperatures documented from other studies (Tourtelot and Rye, 1969; Cochran and others, 2003; He and others, 2005; Dennis and others, 2013) and suggest that the seeps were indeed "cold" seeps. However, the specimens analyzed do not necessarily represent the exact same instant in time, although they all belong to the *B. compressus* Zone (Landman and others, 2018). Differences in temperature observed among the specimens may reflect longer term temporal differences or even seasonal variation recorded in specimens that grew rapidly or secreted shell at different times of the year.

One notable aspect of the $\delta^{18}O$ data is the larger ontogenetic variation in $\delta^{18}O$ (and temperature) in the non-seep specimens versus the seep specimens. This is particularly striking in AMNH 82655 from a seep site, which spans the range of whorl heights in AMNH 108142 and 66330 from non-seep sites, yet lacks the temperature

variation observed in the latter specimens. Variation in $\delta^{18}O$ in *Baculites* has been interpreted as reflecting seasonal variation in water temperature (Fatherree and others, 1998; Tobin and Ellis, 2017). One possibility to explain the difference between the sclerochronological patterns of $\delta^{18}O$ in seep and non-seep specimens is that the non-seep specimens lived in a portion of the water column that was more susceptible to seasonal temperature variation, while the geochemical evidence suggests that seep specimens were living near the bottom for extended periods of time. This near-bottom environment may have experienced less seasonal temperature variation.

A cross plot of $\delta^{13}C$ versus $\delta^{18}O$ reinforces the interpretations of the data as described above (fig. 9). The highlighted gray zone in figure 9 corresponds to the non-seep field of $\delta^{13}C$ values. The range in $\delta^{13}C$ is greater than that of $\delta^{18}O$, and specimens collected at seeps show $\delta^{13}C$ values that depart from the non-seep field in the direction of ^{12}C enrichment. Significantly, the cross-plot shows no relationship between $\delta^{13}C$ and $\delta^{18}O$ that might be expected from alteration, that is, a positive correlation, as documented for WIS ammonites by Cochran and others (2010). This reflects both the well-preserved nature of the shell material selected for this study (figs. 4 and 5) and also the rigorous sample screening by examination of shell microstructure by SEM on every sample analyzed (fig. 6).

Contributions of Carbon from DIC and Metabolic Sources

The differences in $\delta^{13}C$ between the seep and non-seep specimens suggest that the seep environment was isotopically distinct from the non-seep environment and that this difference was manifested as a ^{12}C-enriched signal in the DIC reservoir above the seep. It may also have characterized the $\delta^{13}C$ of organic matter generated in the seep food web that utilized the ^{12}C-enriched DIC. Indeed, *Baculites compressus* may have been feeding on small animals in the water column, such as floating crustacean larvae, as suggested by Kruta and others (2011).

Both metabolic carbon and carbon derived from the DIC reservoir were likely important in controlling the $\delta^{13}C$ of the ammonite shell (McConnaughey and others, 1997; Tobin and Ward, 2015). Following Tobin and Ward (2015), the relationship among these parameters can be expressed as:

$$\delta^{13}C_{shell} = \varepsilon + C_{meta} \times \delta^{13}C_{meta} + (1\text{-}C_{meta}) \times \delta^{13}C_{DIC} \quad (3)$$

where ε is the $\delta^{13}C$ fractionation between aragonite and DIC ($+2.7 \pm 0.6‰$, dominated by HCO_3^-; Romanek and others, 1992), C_{meta} is the fraction of metabolic carbon incorporated into the shell, and $\delta^{13}C_{\text{shell, meta, DIC}}$ are the $\delta^{13}C$ values corresponding to the shell, metabolic carbon, and DIC, respectively. Equation 3 has three unknowns: C_{meta}, $\delta^{13}C_{meta}$, and $\delta^{13}C_{DIC}$. In their study of ammonites and other molluscs from Seymour Island, Antarctica, Tobin and Ward (2015) estimated the value of C_{meta} for ammonites by using values of 0 and 10 percent for C_{meta} of benthic molluscs to determine values of $\delta^{13}C_{DIC}$. They solved equation 3 for C_{meta} for ammonites using the measured ammonite $\delta^{13}C_{shell}$, assuming that $\delta^{13}C_{meta}$ for ammonites was comparable to that of organic material in the siphuncle of modern *Nautilus*, -17 permil (Crocker and others, 1985). A similar value ($-17.4‰$) was measured by Pape (2016) in siphuncular organic material in *Nautilus*, but she also determined $\delta^{13}C$ of the shell-bound organic material to be -14.3 ± 0.7 permil. The values of C_{meta} calculated by Tobin and Ward (2015) for ammonites ranged from 29 percent to 37 percent. One complication in their interpretation of the ammonite $\delta^{13}C$ data is that the section sampled in Seymour Island contains evidence for methane seep deposits and diffuse seepage throughout (Little and others, 2015), and at least some of the isotope values could have been affected by incorporation of ^{12}C-enriched carbon derived from the seeps. As well, Tobin and Ward (2015) studied multiple ammonite

genera, and C_{meta} might have varied among genera as it does in modern bivalve genera.

In an effort to constrain the variables in equation 3 pertinent to the WIS seeps, we use the data of Sessa and others (2015) to estimate C_{meta} for *Baculites*. Sessa and others (2015) measured $\delta^{13}C$ and $\delta^{18}O$ in planktonic and benthic foraminifera, ammonites (*Eubaculites*, which is closely related to *Baculites*, *Discoscaphites*, and *Sphenodiscus*), epifaunal and infaunal bivalves, and gastropods in the Upper Cretaceous Owl Creek Formation of Mississippi. Although this is a different environment and much higher ammonite zone than the *B. compressus* Zone of the U.S. Western Interior of the present study, the rich data set of Sessa and others (2015) permits us to estimate the C_{meta} of *Baculites*. Average $\delta^{13}C$ values of well-preserved specimens of benthic foraminifera (two genera), infaunal bivalves, and *Eubaculites* are (+0.8‰ and +0.9‰), +1.6 permil, and −1.4 permil, respectively. We rearrange equation 3 to solve for $\delta^{13}C_{DIC}$ as a function of $\delta^{13}C_{shell}$, $\delta^{13}C_{meta}$ and C_{meta}:

$$\delta^{13}C_{DIC} = [\delta^{13}C_{shell} - \varepsilon_{aragonite} - (C_{meta} \times \delta^{13}C_{meta})]/[1 - C_{meta}] \qquad (4)$$

Applying equation 4 to the bivalve data of Sessa and others (2015), assuming C_{meta} = 10 percent and $\delta^{13}C_{meta} = -17$ permil, yields $\delta^{13}C_{DIC} = 0.7$ permil. This value is comparable to those measured in the two genera of calcitic benthic foraminifera (0.8‰ and 0.9‰), which approximate the $\delta^{13}C$ of bottom water DIC. Taking $\delta^{13}C_{DIC} = 0.7$ permil and $\delta^{13}C_{meta} = -17$ permil, C_{meta} for specimens of *Eubaculites* in the Owl Creek Formation ($\delta^{13}C_{shell} = -1.4$‰) is ~29 percent (0.29). Interestingly, this value is comparable to the lower of the estimates of Tobin and Ward (2015), although that estimate assumed that the C_{meta} for benthic molluscs was 0 percent.

We can use the value of C_{meta} calculated for *Eubaculites* from the Owl Creek Formation (29%) to place constraints on the $\delta^{13}C$ values of *Baculites compressus* collected at both seep and non-seep WIS sites. However, two interdependent variables remain: $\delta^{13}C_{meta}$ and $\delta^{13}C_{DIC}$ (eqn. 4). The values of both $\delta^{13}C_{DIC}$ and $\delta^{13}C_{meta}$ may have been lower at the seeps than those in the non-seep environment if methane-derived carbon enriched in ^{12}C was imprinted on the DIC and organic matter derived from it. Considering first the non-seep WIS environment (as represented by AMNH 108142 and 66330), $\delta^{13}C_{shell}$ values of −0.6 permil (table 2), coupled with C_{meta} = 29 percent and $\delta^{13}C_{meta} = -17$ permil, produce a calculated value of $\delta^{13}C_{DIC}$ of +2.3 permil.

The mean values of $\delta^{13}C_{shell}$ of seep *Baculites compressus* range as low as −2.7 permil, with individual values (in AMNH 82655) as low as ~ −4.8 permil (tables 2 and A7). The straight lines in figure 10 show the combinations of values (calculated from eqn. 4) of $\delta^{13}C_{DIC}$ and $\delta^{13}C_{meta}$ that produce $\delta^{13}C_{shell}$ values of −2.7 permil and −4.8 permil for C_{meta} = 29 percent. We include a range of $\delta^{13}C_{meta}$ values extending from the value of $\delta^{13}C$ in shell-bound organic matter in modern *Nautlius* (~−15‰; Pape, 2016) to values ~10 permil lower than modern marine $\delta^{13}C$. For values of $\delta^{13}C_{shell}$ of −2.7 permil and $\delta^{13}C_{meta}$ of −17 permil (Crocker and others, 1985), the $\delta^{13}C_{DIC}$ would have been ~−0.7 permil, or about 3 permil lower than the value calculated above from the non-seep *B. compressus* data (+2.3‰). For the same values of $\delta^{13}C_{meta}$ and C_{meta}, $\delta^{13}C_{DIC}$ would have to have been −3.6 permil to produce a value of −4.8 permil for $\delta^{13}C_{shell}$. Thus, these values of $\delta^{13}C_{DIC}$ are ~3 permil to 6 permil lower than the $\delta^{13}C_{DIC}$ calculated from the non-seep specimens. We note that values of $\delta^{13}C_{meta}$ of −30 permil, lower than typical marine organic matter, require $\delta^{13}C_{DIC}$ to be ~+2 to +5 permil (fig. 10). We also consider the possibility that C_{meta} is higher for specimens living at the seeps. As an example, if C_{meta} = 35 percent (and $\delta^{13}C_{meta} = -17$‰), the calculated values of $\delta^{13}C_{DIC}$ would be ~0.8 permil and −2.4 permil for $\delta^{13}C_{shell}$ values of −2.7 permil and −4.8 permil, respectively.

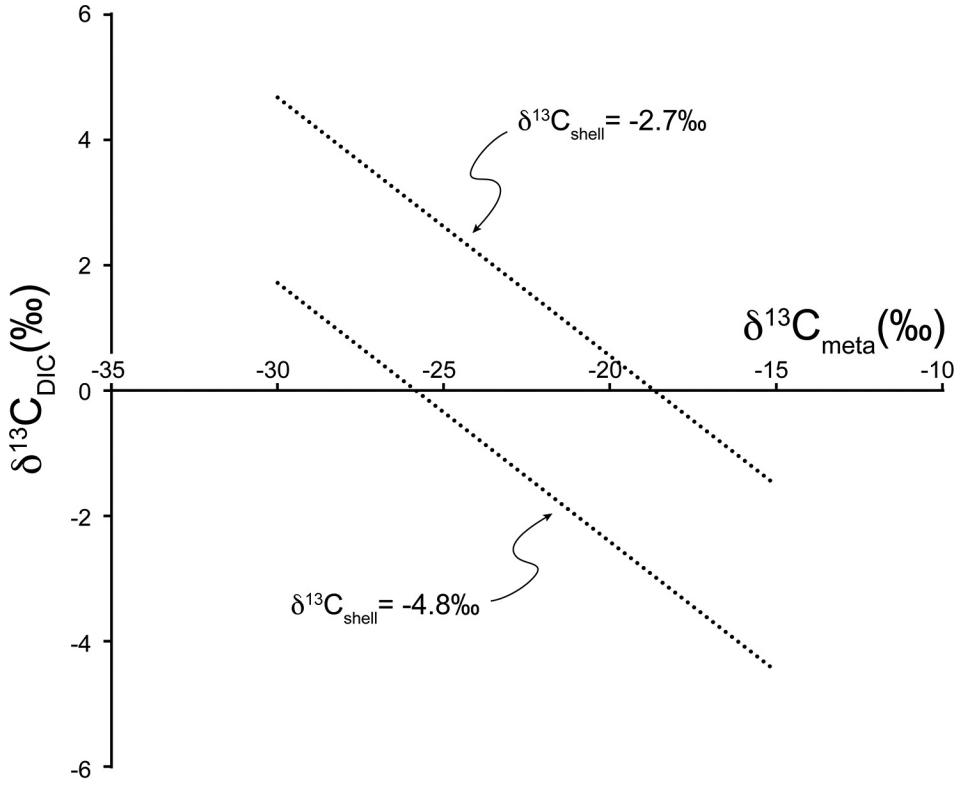

Fig. 10. Relationship between the $\delta^{13}C$ (in ‰ VPDB) of the dissolved inorganic carbon reservoir (DIC) and the $\delta^{13}C$ of metabolic carbon as sources of C to the shell aragonite for $\delta^{13}C_{shell} = -2.7‰$ and $-4.8‰$. The lines are derived from eqn. 4 and show the combination of values of $\delta^{13}C_{DIC}$ and $\delta^{13}C_{meta}$ to produce the observed mean ($\sim -2.7‰$ VPDB) and lowest ($-4.8‰$ VPDB) values of $\delta^{13}C_{shell}$ of *Baculites compressus* collected at WIS seeps, assuming that 29% of the shell C is from metabolic sources. Values are calculated for a range of $\delta^{13}C_{meta}$ from $-15‰$ to $-30‰$. See eqn. 4 in text.

Clues to the $\delta^{13}C_{DIC}$ value of the water above the seeps also come from the low $\delta^{13}C$ values of the authigenic Mg-calcite cemented concretions that occur there (table 1). These suggest that the DIC of the pore fluids from which the carbonates precipitated was characterized by significantly low values of $\delta^{13}C$ ($<<0‰$). The migration of this fluid into the overlying water, as inferred from the anomalous $^{87}Sr/^{86}Sr$ ratios in seep carbonates and ammonite shells (Landman and others, 2012; Cochran and others, 2015), followed by mixing with ambient DIC, suggest that the $\delta^{13}C_{DIC}$ of the water above the seep was likely <0 permil. To produce a value of $\delta^{13}C_{DIC}<0$ permil, the value of $\delta^{13}C_{meta}$ could not have been less than ~ -25 permil (fig. 10). Indeed, if the difference between marine organic C and DIC at the seeps was comparable to the present-day ocean ($\varepsilon \sim -20‰$), then values of seep $\delta^{13}C_{DIC}$ of -0.7 permil to -3.6 permil would suggest that the $\delta^{13}C$ of seep organic matter was ~ -21 permil to -24 permil. These calculations reinforce the idea that the water column above the WIS methane seeps was geochemically distinct from that elsewhere in the WIS.

Methane Seeps as Ammonite Habitats: Paleontological Evidence

In addition to the differences in $\delta^{13}C$ between seep and non-seep specimens of *Baculites compressus*, other data suggest that *B. compressus* and associated ammonites may

have lived at the seeps for extended periods of time. The depth of the seeps, as in the rest of the Western Interior Seaway, did not exceed 100 m, which is entirely consistent with the shallow depth limitations of these ammonites. For example, Hewitt (1996) calculated that the shells of *B. compressus* and those of other ammonites commonly found at seeps and in the WIS could not survive pressures greater than ~10 atm without crushing.

Even though ammonites were mobile animals, they may have been attracted to the seeps due to the rich source of food represented by the high biomass of the localized seep ecosystem (Meehan and Landman, 2016). Indeed, ammonites are abundant at seep deposits in the WIS. Meehan and Landman (2016) reported a total of 23 specimens of *Hoploscaphites nodosus* from a single seep deposit in the *Didymoceras cheyennense* Zone of South Dakota. Landman and others (2013) reported a total of 19 specimens of *Hoploscaphites gilberti* from a single seep deposit from the *Didymoceras nebrascense* Zone of Wyoming. In contrast, ammonites are rare or absent in the shale immediately surrounding the methane seep deposits (Landman and others, 2012). This is not simply a taphonomic phenomenon. Ammonites occur both in the carbonate concretions and loose in the sediments at the seep sites. The shale and carbonate concretions immediately surrounding the seep (10's of meters away) contain few or no ammonites at all (Landman and others, 2012).

The abundance of ammonites varies depending on the seep. For example, in the same area with multiple seep deposits in the *Didymoceras nebrascense*/*Baculites scotti* Zones near Newell, South Dakota, some seeps are more ammonite-rich than others (Meehan and Landman, 2016). In addition, the dominant species of ammonite varies depending on the seep. For example, *Baculites* are generally more abundant than *Hoploscaphites* in most non-seep sites in the WIS, but the reverse is true at seep deposits in the *Baculites baculus* Zone in Niobrara County, Wyoming. Such variation may reflect differences in the flow rates of seep fluids and the extent to which they affected the water column above the seep. This in turn may have affected the development of a seep food web and the abundance of food for molluscs and other organisms. As well, concentrations of oxygen, methane, and hydrogen sulfide in the overlying water column may have played a role, as noted above in the case of the juvenile specimen of *B. compressus* (AMNH 82654).

An additional piece of evidence that ammonites lived at seeps is that in those ammonites in which sexual dimorphism can be recognized, both dimorphs occur in the same seep deposit (fig. 3). At the sites investigated in this study, both dimorphs of *Baculites compressus* are present. In addition, Landman and others (2013) reported 12 macroconchs and 16 microconchs of *Hoploscaphites gilberti* from a single seep deposit from the *Didymoceras nebrascense* Zone of Wyoming. The presence of both dimorphs at these sites implies the existence of a breeding population.

Consistent with the hypothesis that ammonites lived at the seeps is the presence of sublethal and lethal injuries (fig. 11). Sublethal injuries are recognizable as scars on the shell and reflect attacks that occurred during the lifetime of the animal but did not result in death. If the injury occurred at the aperture at the time and affected the mantle, the shell damage usually appears as a groove in the shell, but if it occurred on the body chamber adapical of the aperture at the time, it usually appears as an inflated area ("blister") surrounded by a sharp fracture (Takeda and others, 2015). Lethal injuries are indicated by missing pieces of shell, which tend to occur in the same position on the specimen, for example, at the back of the body chamber, revealing preferred areas of attack. Many of these injuries may have been sustained at the seep sites, suggesting that the ammonites formed an integral part of the seep food web. Indeed, with lethal attacks, it is unlikely that the ammonites were killed elsewhere and floated into the seep, but rather that they lived and died at the site.

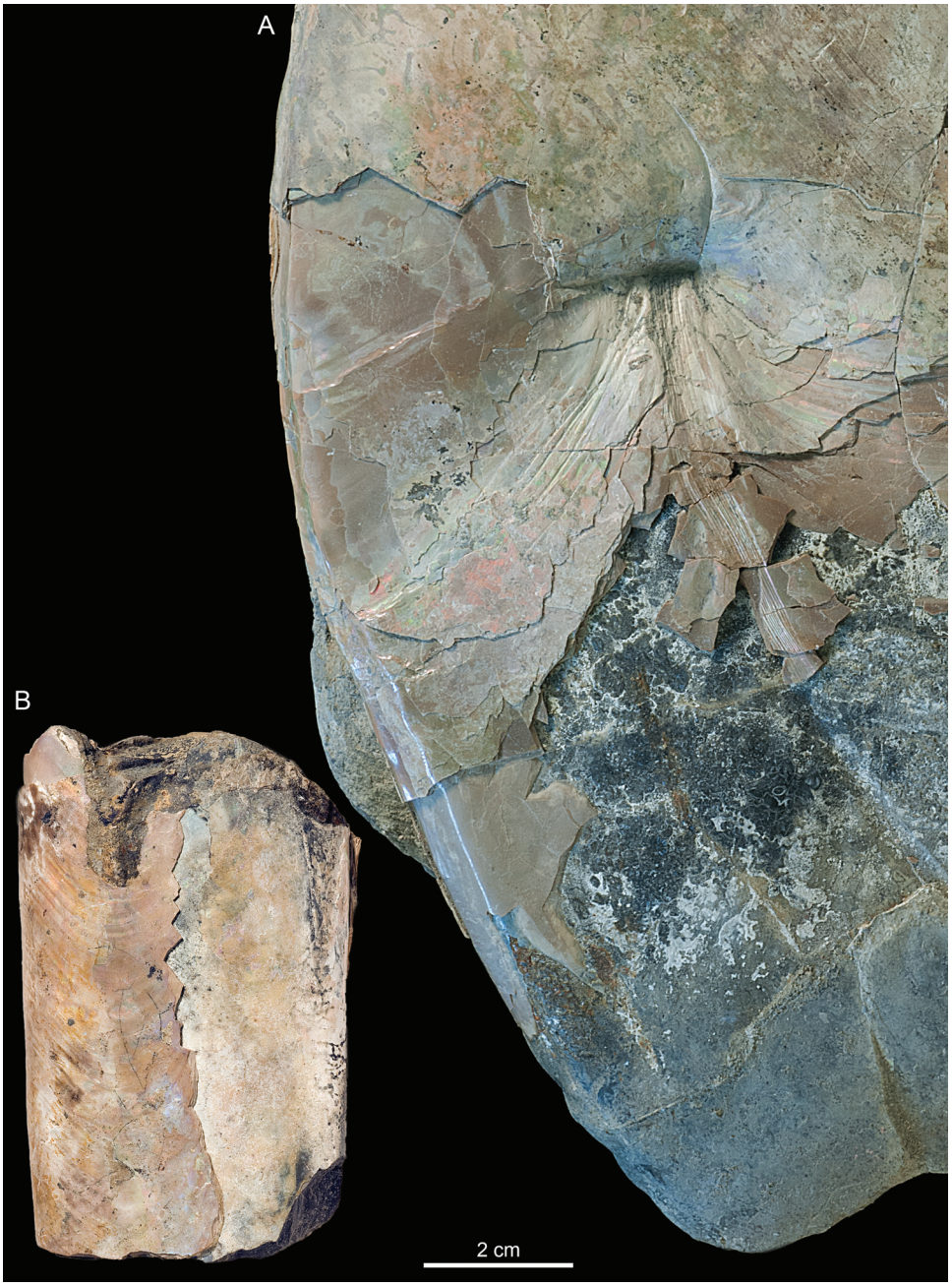

Fig. 11. (A) Healed injuries on the outer flanks of *Placenticeras meeki* Böhm, 1898, AMNH 108168, methane seep deposit, AMNH loc. 3528, Campanian, Pierre Shale, South Dakota. The injury was severe enough to affect the mantle. The adoral direction is toward the bottom of the photo. (B) Broken re-entrant near the aperture of *Baculites compressus* Say, 1820, AMNH 108423, methane seep deposit, AMNH loc. 3528, Campanian, Pierre Shale, South Dakota, probably a result of lethal predation.

Ammonite jaws are also present in seep deposits (figs. 12A–12D). The jaws in ammonites consist of upper and lower mandibles composed of chitin. The lower jaw is also covered with a thin calcareous layer known as the aptychus (Tanabe and others, 2015). Because these structures are very delicate and easily lost after death, their presence suggests that the ammonites lived at the sites and did not float into the area after the animals died. Similarly, seep deposits contain the chitinous hook-like structures attributed to *Hoploscaphties* (figs. 12E–12G). Although the function of these structures is unknown, they are also composed of chitin and are very delicate. These structures could not have survived long distance transport. Their presence suggests instead that the ammonites must have lived and died at the seeps.

These cases of ammonites in seep deposits in the WIS are not exceptional. Ammonites occur in seep deposits throughout the world stretching from the Devonian to the Upper Cretaceous. For example, Little and others (2015) described methane seep deposits in the Upper Cretaceous (Maastrichtian) Snow Hill Island Formation on Snow Hill Island, Antarctica. These seep deposits consist of large cement-rich carbonate bodies filled with the bivalve *Thyasira townsendi*, many in life position, with a concentration of more than $120/m^2$ forming a coquina. They are associated with numerous small ammonites and ammonite fragments, many of which appear to be juveniles. The ammonites belong to the genera *Gunnarites* and *Anagaudryceras*.

Rolin and others (1990) described ammonite-rich seep deposits in lower-middle Oxfordian (Jurassic) black marls of the Terres Noires Formation near Beauvoisin, southeastern France. The carbonate masses are dominated by large infaunal lucinid bivalves, the largest of which is 18 cm long (bivalves comprise up to 30% of the rock). The bivalves are articulated, but not in life position. The ammonites occur in the small irregular concretions on the margins of the masses and include perispinctids and phylloceratids, including numerous *Sowerbyceras*, followed by oppeliids, cardioceratids and pachyceratids. The deposits also contain abundant aptychi (parts of the jaws of the ammonites) and rhyncolites (parts of the jaws of nautilids).

Rolin and others (1990) did a comparative study of the fauna in these seep deposits and at nearby stratigraphically equivalent non-seep sites. Taking into account taphonomic differences (preservation in cemented carbonate concretions versus preservation in black shales), they noted that the fauna in the seep deposits was much more abundant with respect to bivalves, gastropods, ammonites, crustaceans, echinoderms, and fish. They concluded that these animals were living at the seeps. Some of them, such as the bivalves, were restricted to the seeps, whereas the ammonites may have been "*electifs*" opting to remain at the seeps feasting on the abundant food source but equally at home elsewhere.

These occurrences as well as those from the WIS support the hypothesis that ammonite accumulations in seep deposits do not represent dead animals that floated into the sites from elsewhere but rather local accumulations derived from populations living at the sites. In all of the seep deposits described, ammonites are more abundant at the seeps than in the surrounding sedimentary rocks. They are also represented by a range of ontogenetic stages including juveniles and adults. In the deposits in the U.S. Western Interior and southeastern France, seep deposits also contain ammonite jaws and even the hook-like structures attributed to some ammonite taxa. As noted above, both of these kinds of structures could not have survived transport of the ammonites after death.

The fact that ammonites lived at the seeps also bears on previous interpretations of their habitat and mode of life. In the WIS, *Baculites* are usually portrayed as swift swimmers in mid-water (Tsujita and Westermann, 1998). However, if these ammonites spent most of their lives at a single seep site, it suggests instead that they were sedentary animals, at least some of the time, and formed localized populations. The fact that

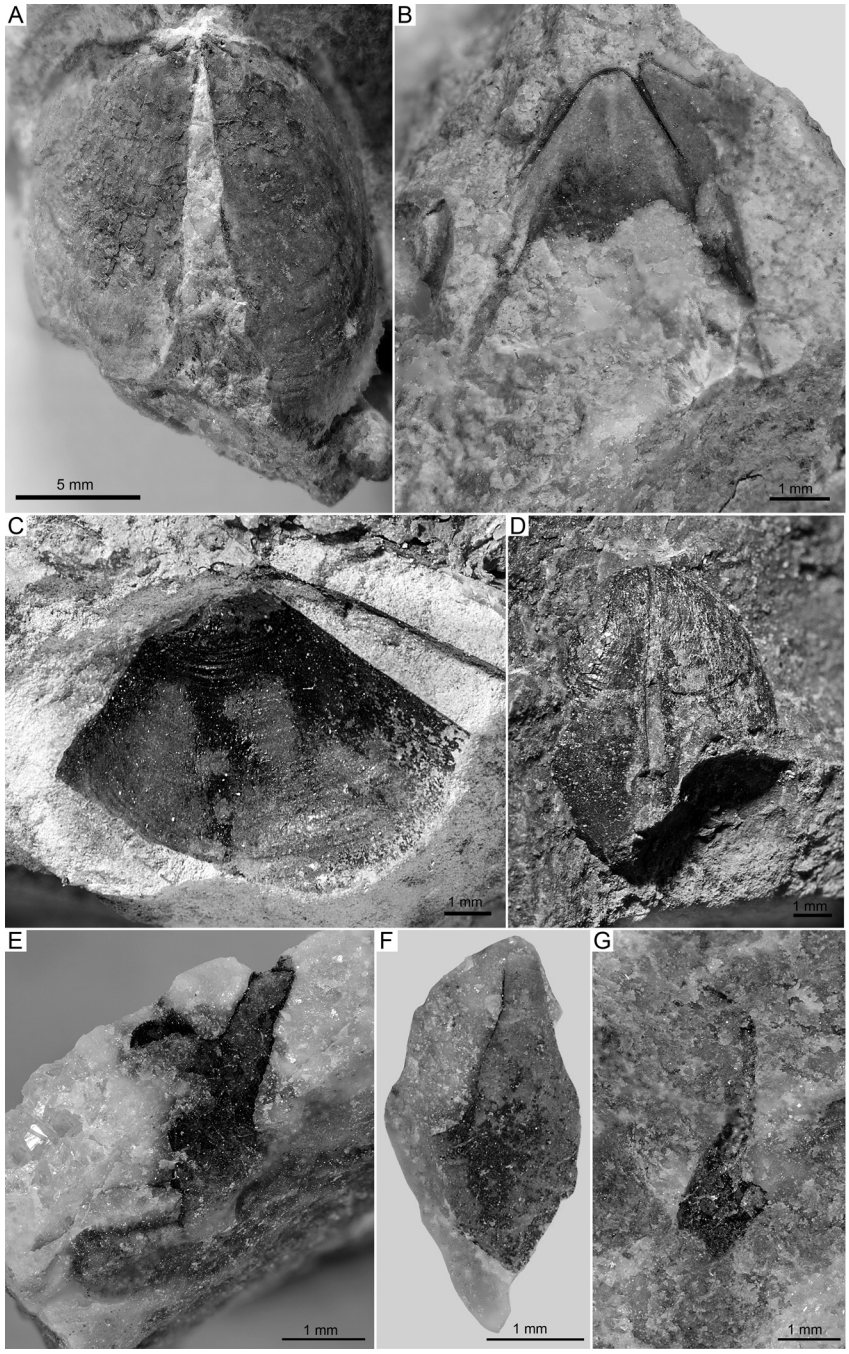

Fig. 12. Jaws and hook-like structures attributed to *Hoploscaphites* from seeps deposits in the Campanian Pierre Shale, South Dakota. (A) Lower jaw showing the midline slit, ventral view, apex on top, AMNH 64532. (B) Upper jaw, apex on top, AMNH 64547. (C) Impression of left side of lower jaw, midline slit on the right, AMNH 63423. (D) Lower jaw showing the midline slit, ventral view, apex on top, AMNH 99198. (E) Hook-like structure showing one of the points projecting to the upper right, AMNH 63530. (F) Hook-like structure with the basal portion exposed on the bottom, AMNH 63531. (G) Hook-like structure with one point complete and one point broken, AMNH 64533.

their shells are imprinted with the seep carbon isotope signal further implies that the animals likely lived within meters of the bottom in contact with seep fluids. They probably exploited a low-energy mode of life, feeding on the abundant zooplankton at the seep. Because many seeps in the WIS occur in clusters (seep fields), the ammonites may have drifted or migrated from one seep to another. These ammonites were not "seep obligate" and occurred elsewhere in the basin. But having stumbled on a seep in early ontogeny, perhaps through olfactory cues, they took full advantage of the abundance of food and biomass associated with these unique environments and spent the rest of their lives at or near the same site.

CONCLUSIONS

Detailed sclerochronological sampling of specimens of *Baculites compressus* collected at fossil methane seep sites in the WIS shows consistently low values of $\delta^{13}C$ that are significantly different from $\delta^{13}C$ in shells of coeval non-seep counterparts. Both metabolic carbon sources and carbon from the dissolved inorganic carbon reservoir (DIC) may have contributed to the $\delta^{13}C$ of seep *B. compressus* shells, but the $\delta^{13}C_{DIC}$ was likely several permil lower than that of non-seep environments in the WIS. These results suggest that the methane seeps acted as habitats for *B. compressus* and that these ammonites spent extended periods of time at the seeps. This isotope evidence is supported by other observations of seep faunal composition, including the abundance of ammonites at seeps compared with the surrounding shale, the presence of sexual dimorphs of the same species, lethal shell injuries, and preserved jaws. Paleotemperatures calculated from the $\delta^{18}O$ values yield comparable results in seep and non-seep specimens of *Baculites compressus* (~21–26 °C) and support the notion that the seeps were "cold" seeps.

A hypothetical reconstruction of the seep ecosystem is shown in figure 13. The organisms pictured have all been collected at seep sites in the WIS (see Landman and others, 2012; Meehan and Landman, 2016), and include nektic, nektobenthic and benthic fauna. Figure 13 illustrates both the living ecosystem and a cross-section of the underlying Pierre Shale sediments showing the preservation of fossils and authigenic carbonates. Processes such as seep fluid transport (inferred from C and Sr isotopes in authigenic carbonate concretions) and methane bubble evolution (inferred from partially cemented burrows and bubble tubes) are also shown. Given the high abundance of seeps in the Late Cretaceous WIS, we hypothesize that they formed an important part of the WIS ecosystem. The relatively shallow water depths of the WIS, the broad extent of seep fields from Montana to Colorado, and the long persistence of seep activity during 6 MY (fig. 1) all suggest that the seeps may have contributed a significant source of methane (and ultimately CO_2) to the Late Cretaceous atmosphere.

ACKNOWLEDGMENTS

We thank Steve Thurston for help in preparing the figures; Shannon Brophy, Alison Rowe, Corinne Myers, Jone Naujokaityte, Remy Rovelli, and Ana Danilova for assistance in the field and stimulating discussion about seeps; Bushra Hussaini and Mary Conway for assistance in organizing and curating the fossils; Morgan Hill, Henry Towbin, and Andrew Smith for assistance in SEM; and Colin Carney and Dyke Andreasen for help and patience in the isotope analyses of samples. Thomas Tobin and an anonymous reviewer provided many helpful comments in their reviews of an earlier manuscript. We thank the landowners in South Dakota for granting us permission to collect samples and specimens from their property. Financial support was provided by the Norman D. Newell Fund at the American Museum of Natural History. JDW was supported by the Lerner-Gray Fund for Marine Research and the Richard Gilder Graduate School (AMNH) via a research fellowship.

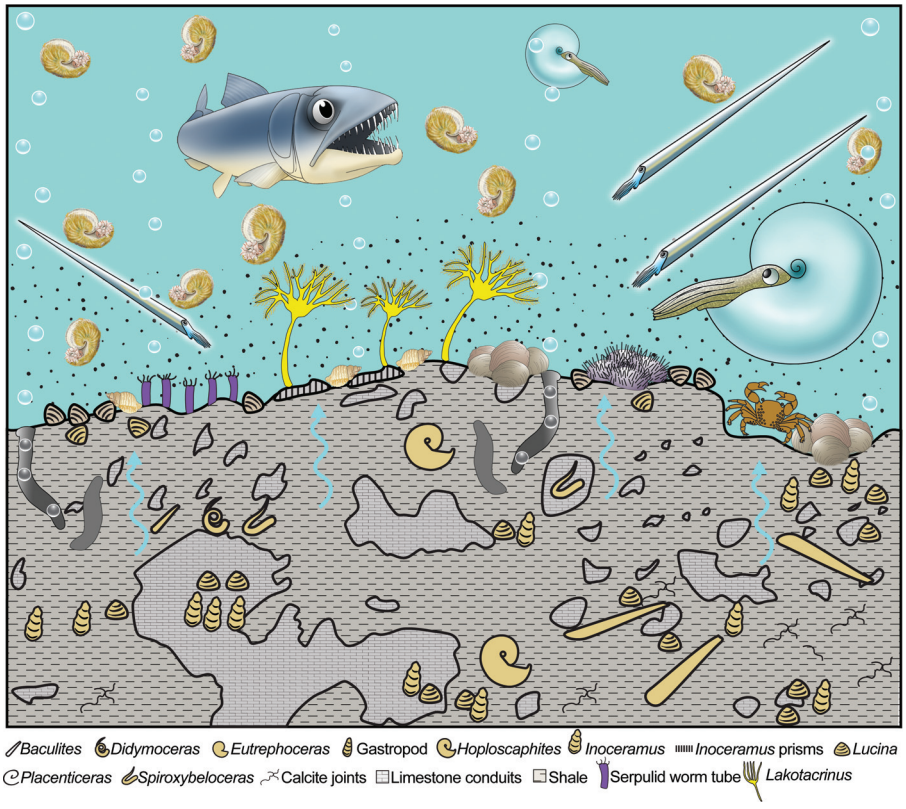

Fig. 13. Reconstruction of a methane seep in the Late Cretaceous Western Interior Seaway (WIS). The organisms shown have all been identified as fossils in seep deposits (Landman and others, 2012). Precipitation of authigenic carbonates as a result of increased carbonate alkalinity due to anaerobic oxidation of methane occurs below and at the sediment-water interface. This provides a hard substrate for crinoids, echinoids, crabs, and other organisms. Tectonically-driven, upward flow of seep fluids provides methane for AOM. Exsolution of dissolved methane produces methane bubbles that can escape the zone of AOM and enter the overlying water. The active redox chemistry at the seeps provides energy for a chemosynthetic-based food web involving organisms from bacteria to fish.

APPENDIX

TABLE A1

Oxygen and carbon isotope composition and calculated temperature for AMNH 64526, Baculites compressus, seep site, AMNH loc. 3545

Sample no.	WH (mm)	PI	$\delta^{13}C$ (‰ VPDB)	$\delta^{18}O$ (‰ VPDB)	Temperature (ºC)
1	45.6	4	-2.1	-1.2	21
2	46.1	4	-2.9	-1.3	21
3	46.3	4	-1.8	-1.3	21
4	46.6	4	-1.7	-1.2	21
5	46.9	4	-2.1	-1.1	20
6	47.4	4	-1.8	-1.1	20
7	47.6	4.5	-2.0	-1.0	20
8	47.8	4.5	-2.0	-1.2	21
9	47.9	4	-2.0	-1.2	21
10	48.2	4	-2.1	-1.1	20
11	48.4	4	-2.2	-1.4	21
12	48.7	4.5	-2.2	-1.2	21
13	48.9	4	-2.3	-1.3	21
14	49.2	4.5	-2.2	-1.2	21
15	49.4	4	-2.2	-1.3	21
16	49.6	4.5	-2.0	-1.3	21
17	49.9	4	-1.8	-1.1	20
18	50.3	4	-2.1	-1.3	21
19	50.4	4.5	-1.9	-1.2	21
20	50.6	4.5	-2.2	-1.2	21
21	50.8	4.5	-1.8	-1.3	21
22	51.1	4.5	-1.8	-1.1	20
23	51.4	4.5	-1.8	-1.4	21
24	51.7	5	-1.8	-1.2	21
25	51.9	5	-1.8	-1.2	21
26	52.1	4	-1.8	-1.3	21
27	52.4	4.5	-1.8	-1.2	21
28	52.6	4.5	-1.7	-1.1	20
29	52.9	4.5	-1.7	-1.2	21
30	53.2	4.5	-1.8	-1.3	21
31	53.3	5	-1.8	-1.2	21
32	53.6	4.5	-1.9	-1.4	21
33	53.8	4	-1.9	-1.3	21
34	53.9	5	-1.9	-1.3	21
35	54.3	4.5	-1.9	-1.3	21
36	54.6	4	-1.9	-1.3	21
37	54.8	4	-2.0	-1.3	21
38	55.2	4.5	-1.8	-1.3	21
39	55.4	4	-1.8	-1.3	21
40	55.7	4.5	-1.9	-1.4	21
41	55.8	4	-2.2	-1.4	21
42	56.1	4	-2.1	-1.4	21
43	56.3	4.5	-2.2	-1.3	21
44	56.5	4	-2.6	-1.4	21
45	56.6	4.5	-2.6	-1.3	21
46	56.8	4	-1.8	-1.2	21

Sample number increases in an apertural direction, as indicated by whorl height (WH). PI = preservation index (Cochran and others, 2010).

TABLE A2

Oxygen and carbon isotope composition and calculated temperature for AMNH 64496, Baculites compressus, seep site, AMNH loc. 3528

Sample no.	WH (mm)	PI	$\delta^{13}C$ (‰ VPDB)	$\delta^{18}O$ (‰ VPDB)	Temperature (ºC)
1	34.1	4	-2.4	-2.3	25
2	34.3	4	-2.3	-2.3	25
3	34.6	3.5	-2.4	-2.3	25
4	35.0	4.5	-2.3	-2.1	24
5	35.4	4.5	-2.7	-2.2	25
6	35.8	3	-3.1	-2.2	25
7	36.0	4.5	-2.8	-2.2	25
8	36.2	4	-2.9	-2.3	25
9	36.4	4.5	-2.7	-2.3	25
10	36.6	4	-2.7	-2.4	26
11	36.8	4	-2.6	-2.5	26
12	37.1	4	-2.6	-2.4	26
13	37.4	4.5	-2.7	-2.5	26
14	37.7	4.5	-2.7	-2.5	26
15	37.8	4	-2.9	-2.6	27
16	38.0	3	-3.4	-2.7	27
17	38.2	4.5	-3.2	-2.7	27
18	38.3	4.5	-2.9	-2.8	27
19	38.5	3.5	-2.9	-2.7	27
20	38.6	4.5	-2.9	-2.7	27
21	38.7	4.5	-2.8	-2.8	27
22	38.9	4.5	-2.9	-2.6	27
23	39.0	4	-2.8	-2.7	27
24	39.1	4.5	-2.8	-2.7	27
25	39.3	3.5	-2.5	-2.8	27
26	39.5	4.5	-2.3	-2.7	27
27	39.8	4.5	-2.2	-2.8	28
28	40.0	3.5	-2.1	-2.8	28
29	40.5	4	-2.6	-2.8	27
30	40.7	4	-2.4	-2.7	27
31	40.8	3.5	-2.1	-2.6	27

Sample number increases in an apertural direction, as indicated by whorl height (WH). PI = preservation index (Cochran and others, 2010).

TABLE A3

Oxygen and carbon isotope composition and calculated temperature for AMNH 108142, Baculites compressus, non-seep site, AMNH loc. 3415

Sample no.	WH (mm)	PI	$\delta^{13}C$ (‰ VPDB)	$\delta^{18}O$ (‰ VPDB)	Temperature (ºC)
1	19.8	3.5	0.4	-1.6	22
2	19.9	4	0.5	-1.8	23
3	20.2	4	-0.04	-1.4	21
4	20.5	4	0.9	-1.6	23
5	20.6	3.5	0.9	-1.6	23
6	20.9	3.5	0.8	-1.6	23
7	21.2	3.5	0.1	-1.3	21
8	21.3	3.5	-0.7	-1.5	22
9	21.6	3.5	-0.1	-1.3	21
10	21.8	3.5	-0.3	-1.2	21
11	22.0	4	0.1	-1.3	21
12	22.4	4	-0.1	-1.4	21
13	22.6	3.5	-0.3	-1.2	21
14	22.9	4	-1.4	-1.3	21
15	23.1	3.5	-0.4	-1.1	20
16	23.4	3.5	-0.7	-1.3	21
17	23.8	4	-0.8	-1.1	20
18	24.1	4.5	-0.9	-1.2	21
19	24.4	3.5	-0.8	-1.2	21
20	24.6	4.5	-1.0	-1.3	21
21	25.0	4	-0.9	-1.2	21
22	25.2	4.5	-1.4	-1.2	21
23	25.5	4	-1.0	-1.2	21
24	25.7	3.5	-1.4	-1.3	21
25	26.0	3.5	-1.1	-1.2	21
26	26.2	3.5	-1.1	-1.1	20
27	26.5	4.5	-1.1	-1.2	21
28	27.0	3.5	-0.7	-1.1	20
29	27.1	4.5	-0.9	-1.0	20
30	27.4	4	-0.7	-1.2	20
31	27.5	4	-1.3	-1.2	21
32	27.8	3.5	-0.1	-1.1	20
33	27.9	3.5	-0.9	-1.1	20
34	28.1	4	-0.6	-1.1	20
35	28.4	4	-0.5	-1.2	20
36	28.8	4.5	-1.2	-1.1	20
37	29.0	4	-1.4	-1.3	21
38	29.3	4.5	-1.4	-1.2	21
39	29.6	4	-0.8	-1.1	20
40	29.8	5	0.5	-1.0	20

Sample number increases in an apertural direction, as indicated by whorl height (WH). PI = preservation index (Cochran and others, 2010).

TABLE A4

Oxygen and carbon isotope composition and calculated temperature for AMNH 66330, Baculites compressus, non-seep site, AMNH loc. 3383 (data from Fatherree and others, 1998)

Sample no.	WH (mm)	$\delta^{13}C$ (‰ VPDB)	$\delta^{18}O$ (‰ VPDB)	Temperature (ºC)
1	26.0	-1.2	-1.4	22
2	27.2	-0.8	-1.5	22
2.5	27.8	-0.4	-1.3	21
3	28.4	0.1	-0.8	19
4	29.6	-0.03	-0.9	19
4.5	30.2	0.1	-1.1	20
5	30.8	-0.2	-0.6	18
5.5	31.4	-0.9	-1.0	20
6	32.0	-0.7	-0.8	19
7	33.2	-0.5	-0.7	18
8	34.4	-0.7	-1.0	20
9	35.6	-0.4	-1.1	20
10	36.8	-0.5	-1.0	20
11	38.0	-0.7	-0.9	19
12	39.2	-0.9	-0.9	19
13	40.4	-0.9	-0.8	19
14	41.6	-1.0	-0.9	19
15	42.8	-0.7	-1.4	22
16	44.0	-1.0	-1.3	21
17	45.2	-0.7	-1.8	23
18	46.4	-0.7	-2.0	24
19	47.6	-1.0	-1.9	23
20	48.8	-1.2	-2.1	25
21	50.0	-0.9	-2.1	24
22	51.2	-1.2	-2.0	24
23	52.4	-1.0	-2.4	26
23.5	53.0	-0.8	-2.5	26
24	53.6	-0.4	-2.5	26
24.5	54.2	-0.5	-2.1	25
25	54.8*	-0.2	-2.6	27
25.5	55.4*	-0.2	-2.5	26
26	56.0*	-0.4	-2.4	26
27	56.6*	-0.1	-2.2	25
28	60.0*	0.0	-2.4	26

Sample number increases in an apertural direction, as indicated by whorl height (WH). The state of preservation was evaluated by Fatherree and others (1998) who noted "unaltered" nacreous tablets. * = estimated.

TABLE A5

Oxygen and carbon isotope composition and calculated temperature for AMNH 64427, Baculites compressus, seep site, AMNH loc. 3528

Sample no.	WH (mm)	PI	$\delta^{13}C$ (‰ VPDB)	$\delta^{18}O$ (‰ VPDB)	Temperature (ºC)
1	21.8	4	-1.0	-2.3	25
2	22.3	4	-1.0	-2.3	25
3	22.4	4	-1.2	-3.5	31
4	22.9	3.5	-0.8	-2.2	25
5	23.7	3	-0.8	-2.1	24
6	23.9	4	-0.7	-1.9	24
7	24.0	3.5	-0.6	-1.8	23
8	24.4	4	-0.8	-1.6	22
9	24.8	3.5	-0.4	-1.4	22
10	25.2	3	-0.7	-2.8	27
11	25.0	4	-0.6	-1.5	22
12	25.2	4.5	-0.9	-1.4	21
13	25.4	3.5	-1.1	-2.7	27
14	25.6	4	-0.9	-1.3	21
15	25.7	4	-0.8	-1.2	20
16	26.0	4	-0.8	-1.1	20
17	26.1	4.5	-1.3	-1.0	20
18	26.4	4.5	-1.6	-2.0	24
19	26.7	4.5	-1.3	-0.9	19
20	26.7	4.5	-1.7	-0.9	19
22	26.9	4	-1.6	-0.8	19
23	27.2	4.5	-2.1	-0.8	19

Sample number increases in an apertural direction, as indicated by whorl height (WH). PI = preservation index (Cochran and others, 2010).

TABLE A6

Oxygen and carbon isotope composition and calculated temperature for AMNH 82656, Baculites compressus, seep site, AMNH loc. 3528

Sample no.	WH (mm)	PI	$\delta^{13}C$ (‰ VPDB)	$\delta^{18}O$ (‰ VPDB)	Temperature (ºC)
A1	38.4	3.5	-2.0	-0.3	16
A3	39.2	3	-3.1	-0.4	17
A4	39.7	3	-2.2	-0.4	17
A5	40.2	3.5	-1.6	-0.2	16
A7	44.8	4	-2.2	-0.2	16
A8	46.2	3.5	-2.7	-0.3	17
A10	46.6	4	-2.8	-0.2	16
A11	46.9	3.5	-2.8	-0.3	17
A12	48.2	3	-2.8	-0.5	17

Sample number increases in an apertural direction, as indicated by whorl height (WH). PI = preservation index (Cochran and others, 2010).

TABLE A7

Oxygen and carbon isotope composition and calculated temperature for AMNH 82655, Baculites compressus, seep site, AMNH loc. 3528

Sample no.	WH (mm)	PI	$\delta^{13}C$ (‰ VPDB)	$\delta^{18}O$ (‰ VPDB)	Temperature (ºC)
A1	24.3	5	-0.1	-0.2	16
A2	25.3	3.5	-0.9	-0.2	16
B1	31.9	4.5	-0.9	-0.2	16
B2	32.0	4.5	-0.7	-0.3	16
B3	32.1	4	-0.9	-0.3	17
B4	32.3	5	-0.9	-0.3	16
C1	33.7	3	-2.0	-0.3	17
C2	34.7	4	-2.2	-0.2	16
C3	35.7	3.5	-1.8	-0.2	16
D1	34.4	3.5	-1.8	-0.2	16
D2	35.1	3	-1.4	-0.1	16
D3	35.8	3	-3.4	-0.2	16
F1	35.6	3.5	-3.2	-0.3	17
F2	36.6	4	-3.1	-0.2	16
F3	37.6	3.5	-2.3	-0.4	17
G1	40.1	3.5	-2.8	-0.2	16
G2	41.1	3.5	-2.8	-0.3	17
G3	42.1	4	-4.4	-0.4	17
H3	49.9	3	-1.6	-0.6	18
H2	50.9	3	-2.5	-0.3	17
I3	51.5	4	-1.8	-0.4	17
I2	51.6	3.5	-2.6	-0.6	18
I1	51.7	4	-3.2	-0.6	18
J2	68.4	3.5	-4.5	-0.2	16
J1	69.4	3	-4.8	0.0	16

Sample number increases in an apertural direction, as indicated by whorl height (WH). PI = preservation index (Cochran and others, 2010).

TABLE A8

Oxygen and carbon isotope composition and calculated temperature for AMNH 82654, Baculites compressus, juvenile, seep site, AMNH loc. 3528

Sample no.	WH (mm)	PI	$\delta^{13}C$ (‰ VPDB)	$\delta^{18}O$ (‰ VPDB)	Temperature (ºC)
1	5.3	4.5-5	1.2	-5.0	37
2	5.7	4.5-5	0.9	-5.0	37
3	6.1	4.5-5	0.5	-3.9	32
4	6.5	4.5-5	-0.4	-4.5	35

Sample number increases in an apertural direction, as indicated by whorl height (WH). PI = preservation index (Cochran and others, 2010).

REFERENCES

Alperin, M. J., and Hoehler, T. J., 2009, Anaerobic methane oxidation by Archaea/sulfate-reducing bacteria aggregates: 1. Thermodynamic and physical constraints: American Journal of Science, v. 309, n. 10, p. 869–957, https://doi.org/10.2475/10.2009.01

Bishop, G. A., and Williams, A. B., 2000, Fossil crabs from Tepee Buttes, submarine seeps of the late Cretaceous Pierre Shale, South Dakota and Colorado, USA: Journal of Crustacean Biology, v. 20, n. 5, p. 286–300, https://doi.org/10.1163/1937240X-90000031

Boetius, A., Ravenschlag, K., Schubert, C. J., Rickert, D., Widdel, F., Gieseke, A., Amann, R., Jørgensen, B. B., Witte, U., and Pfannkuche, O., 2000, A marine microbial consortium apparently mediating anaerobic oxidation of methane: Nature, v. 407, p. 623–626, https://doi.org/10.1038/35036572

Böhm, J., 1898, Über *Ammonites pedernalis* von Buch: Zeitschrift der Deutschen Geologischen Gesellschaft, v. 50, p. 183–201.

Campbell, K. A., 2006, Hydrocarbon seep and hydrothermal vent paleoenvironments and paleontology: Past developments and future research directions: Palaeogeography, Palaeoclimatology, Palaeoecology, v. 232, n. 2–4, p. 362–407, https://doi.org/10.1016/j.palaeo.2005.06.018

Cobban, W. A., and Jeletzky, J. A., 1965, A new scaphite from the Campanian rocks of the Western Interior of North America: Journal of Paleontology, v. 39, n. 5, p. 794–801, http://www.jstor.org/stable/3555306

Cobban, W. A., Merewether, E. A., Fouch, T. D., and Obradovich, J. D., 1994, Some Cretaceous shorelines in the Western Interior of the United States, *in* Caputo, M. V., Petersen, J. A., and Franczyk , K. J., editors, Mesozoic systems of the Rocky Mountain region, USA: Denver, Colorado, Rocky Mountain Section of Society for Sedimentary Geology. p. 393–413.

Cobban, W. A., Walaszczyk, I., Obradovich, J. D., and McKinney, K. C., 2006, A USGS zonal table for the Upper Cretaceous Middle Cenomanian–Maastrichtian of the Western Interior of the United States based on ammonites, inoceramids, and radiometric ages: U.S. Geological Survey Open-File Report 2006-1250, p. 1–46.

Cochran, J. K., Landman, N. H., Turekian, K. K., Michard, A., and Schrag, D. P., 2003, Paleoceanography of the Late Cretaceous (Maastrichtian) Western Interior Seaway of North America: Evidence from Sr and O isotopes: Palaeogeography, Palaeoclimatology, Palaeocology, v. 191, n. 1, p. 45–64, https://doi.org/10.1016/S0031-0182(02)00642-9

Cochran, J. K., Kallenberg, K., Landman, N. H., Harries, P. J., Weinreb, D., Turekian, K. K., Beck, A. J., and Cobban, W. A., 2010, Effect of diagenesis on the Sr, O, and C isotope composition of Late Cretaceous mollusks from the Western Interior Seaway of North America: American Journal of Science, v. 310, n. 2, p. 69–88, https://doi.org/10.2475/02.2010.01

Cochran, J. K., Landman, N. H., Larson, N. L., Meehan, K. C., Garb, M., and Brezina, J., 2015, Geochemical evidence (C and Sr isotopes) for methane seeps as ammonite habitats in the Late Cretaceous (Campanian) Western Interior Seaway: Swiss Journal of Palaeontology, v. 134, n. 2, p. 153–165, https://doi.org/10.1007/s13358-015-0087-9

Crocker, K. C., DeNiro, M. J., and Ward, P. J., 1985, Stable isotopic investigations of early development in extant and fossil chambered cephalopods I. Oxygen isotopic composition of eggwater and carbon isotopic composition of siphuncle organic matter in *Nautilus*: Geochimica et Cosmochimica Acta, v. 49, n. 12, p. 2527–2532, https://doi.org/10.1016/0016-7037(85)90120-6

Davis, R. A., Landman, N. H., Dommergues, J-L., Marchand, D., and Bucher, H., 1996, Mature modifications and dimorphism in ammonoid cephalopods, *in* Landman, N. H., Tanabe, K., and Davis, R. A., editors, Ammonoid Paleobiology: Boston, Springer, Topics in Geobiology, v. 13, p. 463–539, https://doi.org/10.1007/978-1-4757-9153-2_13

Dennis K. J., Cochran J. K., Landman, N. H., and Schrag, D. P., 2013, The climate of the Late Cretaceous: New insights from the application of the carbonate clumped isotope thermometer to Western Interior Seaway macrofossil: Earth and Planetary Science Letters, v. 362, p. 51–65, https://doi.org/10.1016/j.epsl.2012.11.036

Elias, M. K., 1933, Cephalopods of the Pierre Formation of Wallace County, Kansas, and adjacent area: University of Kansas Science Bulletin, v. 21, n. 9, p. 289–363.

Fatherree, J. W., Harries, P. J., and Quinn, T. M., 1998, Oxygen and carbon isotopic "dissection" of *Baculites compressus* (Mollusca: Cephalopoda) from the Pierre Shale (upper Campanian) of South Dakota: Implications for paleoenvironmental reconstructions: Palaios, v. 13, n. 4, p. 376–385, https://doi.org/10.2307/3515325

Gilbert, G. K., and Gulliver, F. R., 1895, Tepee Buttes: Geological Society of America Bulletin, v. 6, n. 1, p. 333–342, https://doi.org/10.1130/GSAB-6-333

Gill, J. R., and Cobban, W. A., 1966, The Red Bird section of the Upper Cretaceous Pierre Shale in Wyoming: U.S. Geological Survey Professional Paper 393-A, p. 1–73.

Grossman, E. L, and Ku, T. L 1986, Oxygen and carbon isotope fractionation in biogenic aragonite: Temperature effects: Chemical Geology, v. 59, n. 1, p. 59–74, https://doi.org/10.1016/0168-9622(86)90057-6

He, S., Kyser, T. K., and Caldwell, W. G. E., 2005, Paleoenvironment of the Western Interior Seaway inferred from $\delta^{18}O$ and $\delta^{13}C$ values of molluscs from the Cretaceous Bearpaw marine Cyclothem: Palaeogeography, Palaeoclimatology, Palaeoecology, v. 217, n. 1–2, p. 67–85, https://doi.org/10.1016/j.palaeo.2004.11.016

Hewitt, R. A., 1996, Architecture and strength of the ammonoid shell, *in* Landman, N. H., Tanabe, K., and Davis, R. A., editors, Ammonoid Paleobiology: New York, Plenum Press, Topics in Geobiology, v. 13, p. 297–339, https://doi.org/10.1007/978-1-4757-9153-2_10

Howe, B., ms, 1987, Tepee buttes: A petrological, paleontological, and paleoenvironmental study of

Cretaceous submarine spring deposits: Boulder, Colorado, University of Colorado at Boulder, Masters thesis, p. 1–218.
Hudson, J. D., and Anderson, T. F., 1989, Ocean temperatures and isotopic compositions through time: Earth and Environmental Transactions of the Royal Society of Edinburgh: Earth Sciences, v. 80, n. 3–4, p. 183–192, https://doi.org/10.1017/S0263593300028625
Hunter, A. W., Larson, N. L., Landman, N. H., and Oji, T., 2016, *Lakotacrinus brezinai* n. gen. n. sp., a new stalked crinoid from cold methane seep deposits in the Upper Cretaceous (Campanian) Pierre Shale, South Dakota, United States: Journal of Paleontology, v. 90, n. 3, p. 506–524, https://doi.org/10.1017/jpa.2016.21
Ivany, L. C., and Artruc, E. G., 2016, Isotope ecology of a giant heteromorph ammonite from Antarctica: Geological Society of America Abstracts, Paper No. 145–4.
Iversen, N., and Jørgensen, B. B., 1985, Anaerobic methane oxidation rates at the sulfate-methane transition in marine sediments from Kattegat and Skagerrak (Denmark): Limnology and Oceanography, v. 30, n. 5, p. 944–955, https://doi.org/10.4319/lo.1985.30.5.0944
Kauffman, E. G., Arthur, M. A., Howe, B., and Scholle, P. A., 1996, Widespread venting of methane-rich fluids in Late Cretaceous (Campanian) submarine springs (Tepee Buttes), Western Interior Seaway, U.S.A.: Geology, v. 24, n. 9, p. 799–802, https://doi.org/10.1130/0091-7613(1996)024<0799:WVOMRF>2.3.CO;2
Kiel, S., Weiser, F., and Titus, A. L., 2012, Shallow-water methane-seep faunas in the Cenomanian Western Interior Seaway: No evidence for onshore-offshore adaptations to deep-sea vents: Geology, v. 40, n. 9, p. 839–842, https://doi.org/10.1130/G33300.1
Knoll, K., Landman, N. H., Cochran, J. K., Macleod, K. G., and Sessa, J. A., 2016, Microstructural preservation and the effects of diagenesis on the carbon and oxygen isotope composition of Late Cretaceous aragonitic mollusks from the Gulf Coastal Plain and the Western Interior Seaway: American Journal of Science, v. 316, n. 7, p. 591–613, https://doi.org/10.2475/07.2016.01
Kruta, I., Landman, N., Rouget, I., Cecca, F., and Tafforeau, P., 2011, The role of ammonites in the Mesozoic marine food web revealed by jaw preservation: Science, v. 331, n. 6013, p. 70–72, https://doi.org/10.1126/science.1198793
Landman, N. H., and Klofak, S. M., 2012, Anatomy of a concretion: Life, death, and burial in the Western Interior Seaway: Palaios, v. 27, n. 10, p. 671–693, https://doi.org/10.2110/palo.2011.p11-105r
Landman, N. H., Kennedy, W. J., Cobban, W. A., and Larson, N. L., 2010, Scaphites of the "*nodosus* Group" from the Upper Cretaceous (Campanian) of the Western Interior of North America: Bulletin of the American Museum of Natural History, n. 342, p. 1–242, https://doi.org/10.1206/659.1
Landman, N. H., Cochran, J. K., Larson, N. L., Brezina, J., Garb, M. P., and Harries, P. J., 2012, Methane seeps as ammonite habitats in the U.S. Western Interior Seaway revealed by isotopic analyses of well-preserved shell material: Geology, v. 40, n. 6, p. 507–510, https://doi.org/10.1130/G32782.1
Landman, N. H., Kennedy, W. J., Cobban, W. A., Larson, N. L., and Jorgensen, S. D., 2013, A new species of *Hoploscaphites* (Ammonoidea: Ancyloceratina) from cold methane seeps in the Upper Cretaceous of the U.S. Western Interior: American Museum Novitates, n. 3781, p. 1–39, https://doi.org/10.1206/3781.2
Landman, N. H., Grier, J. C., Grier, J. W., Cochran, J. K., and Klofak, S. M., 2015, 3-D orientation and distribution of ammonites in a concretion from the Upper Cretaceous Pierre Shale of Montana: Swiss Journal of Paleontology, v. 134, n. 3, p. 257–279, https://doi.org/10.1007/s13358-015-0084-z
Landman, N. H., Grier, J. W., Cochran, J. K., Grier, J. C., Petersen, J. G., and Towbin, W. H., 2017, Nautilid nurseries: Hatchlings and juveniles of *Eutrephoceras dekayi* from the lower Maastrichtian (Upper Cretaceous) Pierre Shale of east-central Montana: Lethaia, v. 51, n. 1, p. 48–74, https://doi.org/10.1111/let.12222
Landman, N. H., Jicha, B. R., Cochran, J. K., Garb, M. P., Brophy, S. K., Larson, N. L., and Brezina, J., 2018, $^{40}Ar/^{39}Ar$ date of a bentonite associated with a methane seep deposit in the upper Campanian *Baculites compressus* Zone, Pierre Shale, South Dakota: Cretaceous Research, v. 90, https://doi.org/10.1016/j.cretres.2018.03.024
Larson, N. L., Jorgensen, S. D., Farrar, R. A., and Larson, P. L., 1997, Ammonites and the other cephalopods of the Pierre Seaway: Tucson, Arizona, Geoscience Press, p. 1–148.
Larson, N. L., Brezina, J., Landman, N. H., Garb, M. P., and Handle, K. C., 2014, Hydrocarbon seeps: Unique habitats that preserved the diversity of fauna in the Late Cretaceous Western Interior Seaway: Unpublished manuscript available at academia.edu/4641897/Hydrocarbon_seeps_unique_habitats
Linzmeier, B. J., Landman, N. H., Peters, S. E., Kozdon, R., Kitajima, K., and Valley, J. W., 2018, Ion microprobe stable isotope evidence for ammonite habitat and life mode during early ontogeny: Paleobiology.
Little, C. T. S., Birgel, D., Boyce, A. J., Crame, J. A., Francis, J. E., Kiel, S., Peckmann, J., Pirrie, D., Rollinson, G. K., and Witts, J. D., 2015, Late Cretaceous (Maastrichtian) shallow water hydrocarbon seeps from Snow Hill and Seymour Islands, James Ross Basin, Antarctica: Palaeogeography, Palaeoclimatology, Palaeoecology, v. 418, p. 213–228, https://doi.org/10.1016/j.palaeo.2014.11.020
McConnaughey, T. A., and Gillikin, D. P., 2008, Carbon isotopes in mollusk shell carbonates: Geo-Marine Letters, v. 28, n. 5–6, p. 287–299, https://doi.org/10.1007/s00367-008-0116-4
McConnaughey, T. A., Burdet, J., Whelan, J. F., and Paull, C. K., 1997, Carbon isotopes in biological carbonates: Respiration and photosynthesis: Geochimica et Cosmochimica Acta, v. 61, n. 3, p. 611–622, https://doi.org/10.1016/S0016-7037(96)00361-4
Meehan, K. C., and Landman, N. H., 2016, Faunal associations in cold-methane seep deposits from the Upper Cretaceous Pierre Shale, South Dakota: Palaios, v. 31, n. 6, p. 291–301, https://doi.org/10.2110/palo.2015.055
Meek, F. B., 1876, A report on the invertebrate Cretaceous and Tertiary fossils of the upper Missouri country: United States Geological Survey of the Territories Report 9, p. 1–629, pls. 1–45.
Meek, F. B., and Hayden, F. V., 1856, Descriptions of new species of Gastropoda and Cephalopoda from the

Cretaceous formations of Nebraska Territory: Proceedings of the Academy of Natural Sciences of Philadelphia, v. 8, p. 70–72.
Metz, C. L., 2010, Tectonic controls on the tectonics and distribution of Late Cretaceous, Western Interior Basin hydrocarbon seep mounds (Tepee Buttes) of North America: The Journal of Geology, v. 118, n. 2, p. 201–221, https://doi.org/10.1086/650181
Owen, D. D., 1852, Report of a geological survey of Wisconsin, Iowa, and Minnesota; and incidentally of a portion of Nebraska Territory made under instructions from the United States Treasury Department: Philadelphia, Pennsylvania, Lippincott, Grambo, 2 vols., p. 1–638.
Palamarczuk, S., and Landman, N. H., 2011, Dinoflagellate cysts from the upper Campanian Pierre Shale and Bearpaw Shale of the U. S. Western Interior: Rocky Mountain Geology, v. 46, n. 2, p. 137–164, https://doi.org/10.2113/gsrocky.46.2.137
Pape, E., ms, 2016, Biogeochemical evidence for chemosymbiosis in the fossil record: Leeds, United Kingdom, The University of Leeds, Ph. D. thesis, p. 1–299, http://etheses.whiterose.ac.uk/id/eprint/16118
Peckmann, J., and Thiel, V., 2004, Carbon cycling at ancient methane-seeps: Chemical Geology, v. 205, n. 3–4, p. 443–467, https://doi.org/10.1016/j.chemgeo.2003.12.025
Petersen, S. V., Tabor, C. R., Lohmann, K. C., Poulsen, C. J., Meyer, K. W., Carpenter, S. J., Erickson, J. M., Matsunaga, K. K. S., Smith, S. Y., and Sheldon, N. D., 2016, Temperature and salinity of the Late Cretaceous Western Interior Seaway: Geology, v. 44, n. 11, p. 903–906, https://doi.org/10.1130/G38311.1
Rolin, Y., Gaillard, C., and Roux, M., 1990, Ecologie des pseudobiohermes des Terres Noires jurassiques liés à des paléo-sources sous-marine. Le site oxfordien de Beauvoisin (Drôme, Bassin du sud-Est, France): Palaeogeography, Palaeoclimatology, Palaeoecology, v. 80, n. 2, p. 79–105, https://doi.org/10.1016/0031-0182(90)90123-O
Romanek, C. S., Grossman, E. L., and Morse, J. W., 1992, Carbon isotope fractionation in synthetic aragonite and calcite: Effects of temperature and precipitation rate: Geochimica et Cosmochimica Acta, v. 56, n. 1, p. 419–430, https://doi.org/10.1016/0016-7037(92)90142-6
Rowe, A. J., Landman, N. H., Garb, M. P., and Witts, J. D., 2017, Habitat of juvenile ammonites at methane seeps in the Late Cretaceous Western Interior Seaway, Paper No. 380-7: Geological Society of America Abstracts with Programs, v. 49, n. 6, https://doi.org/10.1130/abs/2017AM-303521
Rowe, A. J., Landman, N. H., Garb, M. P., and Witts, J. D., 2018, Habitat of juvenile ammonites at methane seeps in the Late Cretaceous Western Interior Seaway: 10th International Symposium, "Cephalopods-Present and Past", Program and Abstracts, p. 96.
Say, T., 1820, Observations on some species of zoophytes, shells, &c. principally fossil: American Journal of Science and Arts, v. 2, n. 2, p. 34–45.
Shackleton, N. J., and Kennett, J. P., 1975, Paleotemperature history of the Cenozoic and initiation of Antarctic glaciation: Oxygen and carbon isotope analyses in DSDP sites 277, 279 and 281: Initial Reports of the Deep-Sea Drilling Program, v. 29, p. 743–755, https://doi.org/10.2973/dsdp.proc.29.117.1975
Sessa, J. A., Larina, E., Knoll, K., Garb, M., Cochran, J. K., Huber, B. T., MacLeod, K. G., and Landman, N. H., 2015, Ammonite habitat revealed via isotopic composition and comparisons with co-occurring benthic and planktonic organisms: Proceedings of the National Academy of Sciences of the United States of America, v. 112, n. 51, p. 15562–15567, https://doi.org/10.1073/pnas.1507554112
Shapiro, R., and Fricke, H., 2002, Tepee Buttes: Fossilized methane seep ecosystems: Geological Society of America Field Guide 3, p. 94–101, https://doi.org/10.1130/0-8137-0003-5.94
Takeda Y., Tanabe K., Sasaki T., and Landman N. H., 2015, Durophagous predation on scaphitid ammonoids in the Late Cretaceous Western Interior Seaway of North America: Lethaia, v. 49, n. 1, p. 28–42, https://doi.org/10.1111/let.12130
Tanabe K., Kruta, I., and Landman, N., 2015, Ammonoid buccal mass and jaw apparatus *in* Klug, C., Korn, D., DeBaets, K., Kruta, I., and Mapes, R. H., editors, Ammonoid Paleobiology-From Anatomy to Paleoecology: New York, Springer, Topics in Geobiology, v. 43, p. 429–484.
Tobin, T., and Ellis, N. M., 2017, Stable isotope sclerochronology of *Baculites* reveals potential growth rate estimates, Paper No. 307-5: Geological Society of America Abstracts with Programs, v. 49, n. 6, https://doi.org/10.1130/abs/2017AM-300114
Tobin, T. S., and Ward, P. D., 2015, Carbon isotope ($\delta^{13}C$) differences between Late Cretaceous ammonites and benthic mollusks from Antarctica: Palaeogeography, Palaeoclimatolology, Palaeoecology, v. 428, p. 50–57, https://doi.org/10.1016/j.palaeo.2015.03.034
Tourtelot, H. A., and Rye, R. O., 1969, Distribution of oxygen and carbon isotopes in fossils of Late Cretaceous age, Western Interior region of North America: Geological Society of America Bulletin, v. 80, n. 10, p. 1903–1922, https://doi.org/10.1130/0016-7606(1969)80[1903:DOOACI]2.0.CO;2
Tsujita, C. J., and Westermann, G. E. G., 1998, Ammonoid habitats and habits in the Western Interior Seaway: A case study from the Upper Cretaceous Bearpaw Formation of southern Alberta, Canada: Palaeogeography, Palaeoclimatology, Palaeoecology, v. 144, n. 1–2, p. 135–160, https://doi.org/10.1016/S0031-0182(98)00090-X
Vidal, E. A. G., Villanueva, R., Andrade, J. P., Gleadall, I. G., Iglesias, J., Koueta, N., Rosas, C., Segawa, S., Grasse, B., Franco-Santos, R. M., Albertin, C. B., Caamal-Monsreal, C., Chimal, M. E., Edsinger-Gonzales, E., Gallardo, P., Le Pabic, C., Pascual, C., Roumbedakis, K., and Wood, J., 2014, Cephalopod culture: Current status of main biological models and research priorities, *in* Vidal, E. A. G., editor, Advances in Cephalopod Science- Biology, ecology, cultivation and fisheries: New York, Elsevier, Advances in Marine Biology, v. 67, p. 1–98, https://doi.org/10.1016/B978-0-12-800287-2.00001-9
Whitfield, R. P., 1877, Preliminary report on the paleontology of the Black Hills, containing descriptions of new species of fossils from the Potsdam, Jurassic, and Cretaceous formations of the Black Hills of Dakota: U.S. Geographical and Geological Survey of the Rocky Mountain Region, p. 1–49, https://doi.org/10.5962/bhl.title.55132